Published in final edited form as:
Bioconjug Chem. 2012 December 19; 23(12): 2403–2416. doi:10.1021/bc3004342.

Design, synthesis and X-ray analysis of a glycoconjugate bound to *Mycobacterium tuberculosis* Antigen 85C

Diaa A. Ibrahim[1], **Julie Boucau**[2], **Daniel Lajiness**[2], **Sri Kumar Veleti**[2], **Kevin R. Trabbic**[2], **Samuel S. Adams**[2], **Donald R. Ronning**[2,*], and **Steven J. Sucheck**[2,*]

[1]National Organization for Drug Control & Research, Cairo, Gizaa, Egypt

[2]Department of Chemistry, The University of Toledo, 2801 W. Bancroft Street, Toledo, Ohio 43606, USA

Abstract

Tuberculosis (TB) is a global health threat with nearly 500,000 new cases of multidrug-resistance TB estimated to occur every year, so new drugs are desperately needed. A number of current antimycobacterial drugs work by interfering with the biosynthesis of key components of the mycolylarabinogalactan (mAG). In light of this observation, other enzymes involved in the synthesis of the mAG should also serve as targets for antimycobacterial drug development. One potential target is the Antigen 85 (Ag85) complex, a family of mycolyltransferases that are responsible for the transfer of mycolic acids from trehalose monomycolate (TMM) to the arabinogalactan. Virtual thiophenyl-arbinoside conjugates were docked to antigen Ag85C (PDB code: 1va5) using Glide. Compounds with good docking scores were synthesized by a Gewald synthesis followed by linking to 5-thioarabinofuranosides. The resulting thiophenyl-thioarabinofuranosides were assayed for inhibition of mycoyltransferase activity using a 4-methylumbelliferyl butyrate fluorescence assay. The conjugates showed K_i values ranging from 18.2 to 71.0 μM. The most potent inhibitor was soaked into crystals of *Mycobacterium tuberculosis* antigen 85C and the structure of the complex determined. The X-ray structure shows the compound bound within the active site of the enzyme with the thiophene moiety is positioned in the putative α-chain binding site of TMM and the arabinofuranoside moiety within the known carbohydrate-binding site as exhibited for the Ag85B-trehalose crystal structure. Unexpectedly, no specific hydrogen bonding interactions are being formed between the arabinofuranoside and the carbohydrate-binding site of the active site suggesting that the binding of the arabinoside within this structure is driven by shape complementarily between the arabinosyl moiety and the carbohydrate binding site.

Introduction

Tuberculosis (TB) is a global health threat with nearly 500,000 new cases of multidrug-resistant TB (MDF-TB) estimated to occur every year. More concerning is that since 2006, strains of extensively drug-resistant TB (XDR-TB), estimated to be 4% of MDR-TB, have been reported in over 50 countries. It is also estimated that 30–40% of XDR-TB is

Corresponding Author, Prof. Steven J. Sucheck, Department of Chemistry, The University of Toledo, 2801 W. Bancroft Street, Toledo, Ohio 43606, USA, phone, 419-530-1054, Fax: (+1) 419-530-1990, steve.sucheck@uToledo.edu, For D.R.R.: phone, 419-530-1585; Donald.Ronning@UToledo.edu.

Supporting Information.
^{1}H and ^{13}C spectra for compounds **2a–2d, 3a–3d, 4a, 4b, 5, 7–9, 11, 12c, 12d, 13a–d, 14**, HRMS for compound **14**. The material is available free of charge via internet at http://pubs.acs.org.

The authors declare no competing financial interest.

untreatable with the current antitubercular drug repertoire.[1] Based on this it is clear new approaches to treating the disease are needed. Several of the current drugs used to treat TB work by interfering with mycobacterial cell wall synthesis.[2] Contained within the structure of the cell is a unique macromolecular structure called the mycolylarabinogalactan (mAG), which is composed of the arabinogalactan (AG) and mycolic acids.[3] The structure serves as a protective barrier for the organism and limits the diffusion of hydrophobic and hydrophilic drugs.[4]

A number of antimycobacterial drugs; e.g. ethambutol,[5,6] isoniazid[7] and ethionamide,[8] work by interfering with the biosynthesis of key components of the mAG. In light of this observation, other enzymes involved in the synthesis of the mAG may also serve as targets for antimycobacterial drug development. One potential target that has attracted some attention is Antigen 85 complex (Ag85). Ag85 represents a family (Ag85A, Ag85B and Ag85C) of homologous mycolyltransferases that are responsible for the synthesis of trehalose-6,6´-dimycolate (TDM) from trehalose-6-monomycolate (TMM)[9,10,11,12] and for transfer of mycolic acids from TMM to the arabinogalactan (AG).[13,14] Results from inhibitor studies suggest that Ag85 is essential for bacterial viability. For example, 6-azido-6-deoxytrehalose, a known inhibitor of Ag85s, has been shown to completely inhibit the growth *Mycobacterium aurum* a surrogate for *Mycobacterium tuberculosis*.[15] Other studies which support the essential nature of Ag85 include the use of Ag85-specific antisense oligonucleotides which were shown to reduce *Mycobacterium tuberculosis* growth as well significantly enhance bacterial sensitivity to isoniazid.[16,17] Similarly, an Ag85A knockout strain of *Mycobacterium smegmatis* exhibits increased sensitivity to drugs that target peptidoglycan biosynthesis, i.e. vancomycin and imipenem.[18]

A variety of putative Ag85 inhibitors have been described. For example, alkyl phosphonates[19] expected to mimic the tetrahedral intermediate of Ag85s were shown to be active against *Mycobacterium avium* and inhibited mycolyltransferase activity.[20] Other examples include trehalose-based substrate analogs that contain aliphatic chains which showed activity against *Mycobacterium smegmatis*,[21] and related compounds consisting of 6,6´-bis(sulfonamido) and *N*,*N*´-dialkylamino derivatives active against *Mycobacterium tuberculosis* and *Mycobacterium avium*.[22] Further, a fluorophosphonate derivative of trehalose was shown to form a covalent adduct with the active site serine of *M. tuberculosis* Ag85C.[23] More recently we have found arabinofuranoside-based substrate analogs containing S-alkyl chains (Figure 2) that inhibited the growth of *Mycobacterium smegmatis*;[24,25,26] however, the latter compounds did not inhibit acyltransferase activity using our recently developed colorimetric acyltransferase assay.[27] On the other hand, ester derivatives of arabinofuranosides showed weak (mM) inhibitory activity against Ag85C but were inactive in cell-based assays.[28] In light of this data we thought it was necessary to identify more potent Ag85 inhibitors.

The crystal structures of secreted forms of Ag85A,[29] Ag85B,[30,31] and Ag85C[29,32,33] from *Mycobacterium tuberculosis* have all been determined. The structures reveal an α/β-hydrolase fold, with a catalytic triad formed by Ser124, Glu228 and His260 (Ag85C numbering). The carbohydrate binding site is highly conserved between the three acyltransferases. Near the catalytic triad is a binding site for the carbohydrate moiety with a negative electrostatic potential, as well as a hydrophobic tunnel, well suited to accommodate the shorter α-branch of the mycolyl moiety. Additionally, a nearby shallow cleft possessing hydrophobic character may bind the longer β-branch of the mycolyl moiety. However, it seems more likely the β-branch of the mycolyl moiety will remain embedded in the mycobacterial outer membrane during the mycolyltransfer reaction. According to the proposed mechanism of the catalytic mycolyl transfer reaction, Ser124 attacks the carboxyl carbon of TMM to give a mycolyl-enzyme intermediate and free trehalose. In the next step,

the 6-OH group of a second TMM molecule attacks the carboxylate carbon of the acyl-enzyme intermediate to produce TDM. Both, the acylation and deacylation steps proceed via a high-energy tetrahedral transition state[33]. In the case of the formation of the mAG, the terminal and penultimate primary hydroxyl groups of arabinan serve as acyl acceptors, Figure 1. Recombinant Ag85C has been shown to catalyze this reaction *in vitro*[34]. Based on this model and the available crystallographic data, we envisioned conjugates that would contain both a rigid, drug-like moiety, that could mimic the affinity of the mycolyl moiety and could also be conjugated to a fragment of the arabinan for selectivity, Figure 2. We reasoned the carbohydrate component of compounds could occupy the carbohydrate binding site on Ag85s and provide specificity while a hydrophobic component could occupy the pocket leading into the tunnel proposed to accommodate the α-branch of the mycolyl moiety. The main difficulty in this endeavor would be to select an appropriate motif that could accommodate at least a portion of the putative mycolyl moiety binding site. Our interests were drawn toward 2-amino-4,5,6,7-tetrahydrobenzo[*b*]thiopenes due to their structural similarity with ebselen (Figure 2). We have identified the latter compound as a nM inhibitor of Ag85s via the screening of the NIH Clinical Collection.[35] The ability of this motif to accommodate the putative binding pocket of mycolyl moiety was confirmed by a docking strategy. Once identified, we noted the 2-amino-4,5,6,7-tetrahydrobenzo[*b*]thiophene had been used extensively as a scaffold for enzyme inhibitor development.[36,37,38,39,40] We have previously disclosed the structure of **1a** (Scheme 1),[41,42] and it is important to note, closely related, 2-amino-4,5,6,7-tetrahydrobenzo[*b*]thiophene-3-carbonitrile (**1b**, Scheme 1) has been independently identified as a binder of Ag85C using an ^{15}N-HSQC NMR spectroscopy-based fragment screening protocol.[43,44] The resulting thiophene was found to selectively inhibit the growth of *M. smegmatis* with an MIC of 50–100 μg/mL.[39] More recently, 2-amino-6-propyl-4,5,6,7-tetrahydro-1-benzothiophene-3-carbonitrile (I3-AG85, Figure 2) was identified as a second eneration inhibiter with MICs of 100 μg/mL against *M. tuberculosis*. The I3-AG85 reduced survival of *M. tuberculosis* inside macrophages and at a 100 μM concentration. The compound inhibited the growth of 7 MDR and 3 XDR *M. tuberculosis* strains at 200 μM or lower. Finally, I3-AG85 was shown to inhibit the synthesis of TDM. The generalized structures, which we explored in docking studies, are shown in Figure 2.

Experimental Procedures

Biological Methods

K_M determination for 4-MUB—Ag85C was purified as described previously.[27] All assays were performed under atmospheric pressure at 37 °C in a 384-well format on a Synergy H4 Hybrid Multi-Mode Microplate Reader (Biotek). All 4-methylumbelliferyl butyrate (4-MUB) stock solutions were made stored in 100% DMSO at −20 °C. Excitation and emission wavelengths, 365 nm and 450 nm, respectively, were used to monitor the production of the 4-methylumbelliferone (4-MU) at 20 s intervals for 30 minutes. For each reaction, a master mix was made consisting of: 600 nM Ag85C, 10 mM trehalose, and an appropriate volume of 20 mM bis(2-hydroxyethyl)amino-tris(hydroxymethyl)methane (Acros Organics) for an overall reaction volume of 50 μL. 0.5 μL of 4-MUB was added from each corresponding stock solution to reach the desired substrate concentration (25–400 μM). The data were normalized using negative controls where no Ag85C was added. The background fluorescence from the negative control was subtracted from the intensities measured from the enzyme-catalyzed reaction. To correlate relative fluorescence intensity with the amount of product, the fluorescence of 4-MU (1–1000 nM) was determined using reaction conditions. RFU/min rates from the enzyme-catalyzed reaction were directly correlated to the amount of 4-MU produced per minute using the equation for the line of

best fit, using Microsoft Excel. GraphPad Prism 5 software was used to determine Michelis-Menten parameters via non-linear regression analysis.

Inhibition assays—All stock solutions for each compound were made and stored in 100% DMSO. Excitation and emission scans of each compound to be tested were conducted to avoid regions of overlap with 4-methylumbelliferone. The excitation and emission wavelengths used for each compound were: SA-1: λ_{ex} = 320 nm, λ_{em} = 500 nm; KT-1–189: λ_{ex} = 380 nm, λ_{em} = 500 nm; DI-1: λ_{ex} = 380 nm, λ_{em} = 500 nm; DI-2: λ_{ex} = 320 nm, λ_{em} = 450 nm. All fluorescence intensities were determined at 20 second intervals over 30 min. The identities and concentrations of the reaction components used for determining the K_M were employed in these reactions as well; however, the 4-MUB concentration was held constant at 100 μM. 0.5 μL of each tested inhibitor was added from its corresponding stock solution to give final concentrations ranging from 20 μM to 320 μM. Inhibition was determined by comparing the relative rate of the reaction performed with inhibitor against a reaction that contained no inhibitor (v_i'/v_i, where v_i' and v_i are steady state rates with and without inhibitor, respectively). The equilibrium dissociation constant (K_i) for each inhibitor was obtained by fitting the data into the equation below using Prism:

$$\frac{v_i'}{v_i} = \frac{K_M + [S]}{K_M + [S] + \frac{K_M + [I]}{K_i}}$$

K_M is the Michelis-Menten constant for 4-MUB; [S] and [I] are the concentrations of 4-MUB and inhibitor, respectively.

Protein crystallization, diffraction, and model building—The Ag85C crystals were obtained using the hanging drop method where 1 μL of purified Ag85C was combined with 1 μL of the well solution containing 0.3 M ammonium sulfate and 0.1 M sodium acetate. These crystals were prepared for X-ray diffraction studies by adding 1 μL of a 10.7 mM solution of **13a** dissolved in an 80% v/v solution of DMSO to the 2 μL crystallization drop. These crystals were incubated at 16 °C for 2 days prior to data collection. Crystals were cryoprotected by adding glycerol directly to the drop containing the Ag85C crystal and **13a**. Diffraction data were collected at the LS-CAT beamline at the Advanced Photon Source using a wavelength of 0.97856 Å. Data were reduced using HKL2000.[45] Molecular replacement was performed using EPMR.[46] Manual model building was performed using Coot.[47] Refinement, building of **13a**, and addition of water molecules was performed using Phenix.[48,49] Glycerol molecules were manually fit to F_o-F_c density using Coot.

Kirby-Bauer disk diffusion assay—Disk diffusion assays were adapted from methods outlined by the NCCLS and Wang *et al.*[21,50] *Mycobacterium smegmatis* ATCC 14468 was inoculated into Middlebrook 7H9 containing 0.2% glycerol and ADC enrichment, respectively. The inocula were incubated for approximately 48 hours at 37.5°C at 160 rpm. The bacteria were plated on agar (Lennox or Middlebrook 7H10 containing 0.5% glycerol and OADC Enrichment) using sterile cotton-tipped applicators. Aliquots (10 μL) of arabinose derivatives dissolved in DMSO (20 mg/mL) and INH (500 μg/mL) were applied to 6 mm diameter sterile paper disks. The plates were incubated at 37°C for 24 hours and then analyzed.

Synthetic Methods

Ethyl 2-Amino-4,5,6,7-tetrahydrobenzo[*b*]thiophene-3-carboxylate (**1a**). Cyclohexanone (30.0 mL, 290 mmol), sulfur (9.30 g, 290 mmol), *N*-ethylmorpholine (25.2 mL, 200 mmol) and ethanol (320 mL) were combined in a round bottom flask and stirred at room

temperature. After 3 h of continuous stirring the reaction was complete and filtered to remove sulfur. The solvent was evaporated under reduced pressure. The product was extracted with 200 mL of methanol and crystallized by adding 100 mL of water to the methanol solution. The crystals were filtered and rinsed with cold 1:1 methanol-water: yield = 17.6 g (27%); m.p. = 117–119 °C (Lit: [51] 113–117 °C); R_f = 0.55 (4:1 hexanes-ethyl acetate); mass spectrum (ESIMS), *m/z* = 226 $(M+H)^+$, $C_{11}H_{106}NO_2S$ requires 226.

2-Amino-4,5,6,7-tetrahydrobenzo[*b*]thiophene-3-carbonitrile (**1b**). Cyclohexanone (30.0 mL, 290 mmol), malonitrile (19.8 g, 290 mmol), sulfur (9.30 g, 290 mmol), and 25.2 mL of *N*-ethylmorpholine (25.2 mL, 200 mmol) were combined in a round bottom flask and stirred at room temperature. After 3 h of continuous stirring the reaction was complete and filtered to remove sulfur. The solvent was evaporated under reduced pressure and the product was extracted by 200 mL of methanol. The product was crystallized by adding 100 mL of water to the methanol solution. The crystals were filtered and rinsed with a solution of cold 4:1 methanol -water: yield = 17.0 g (33%); m.p. = 147–149 °C (Lit:[52] 147 °C); R_f = 0.35 (9:1 hexane-ethyl acetate); mass spectrum (ESIMS), *m/z* = 179 $(M+H)^+$, $C_9H_{11}N_2S$ requires 179.

Ethyl 2-[(2-chloroacetyl) amino]-4,5,6,7-tetrahydrobenzo[*b*]thiophene-3-carboxylate (**2a**).[53] Compound (**1a**) (0.500 mg, 2.2 mmol) was treated with chloroacetyl chloride (0.35 mL, 4.4 mmol) in chloroform (5 mL) and reaction was refluxed for 3 h. The reaction was analyzed for completion by TLC with 9:1 hexanes – ethyl acetate. The reaction solution was concentrated under reduced pressure and the residue crystallized from chloroform-hexanes: yield 0.231 g (34%); m.p. = 118–121 °C (Lit:[54] 115–117 °C); R_f = 0.49 (9:1 hexanes-ethylacetate); ^{1}H NMR ($CDCl_3$, 400 MHz): δ1.39 (t, *J* = 7.2 Hz, 3H), 1.79–1.81 (m, 4H), 2.66 (t, *J* = 4.4 Hz, 2H), 2.79 (t, *J* = 5.2 Hz, 2H), 4.26 (s, 2H), 4.36 (q, *J* = 7.2 Hz, 2H), 12.14 (br. s, 1H, NH); mass spectrum (ESIMS), *m/z* = 324 $(M+Na)^+$, $C_{13}H_{16}ClNO_3S$ requires 324.

Ethyl 2-[(4-chlorobutanoyl) amino]-4,5,6,7-tetrahydrobenzo[*b*]thiophene-3-carboxylate (**2b**). Compound **1a** (1.13 g, 5.00 mmol), triethyl amine (2.10 mL, 15.0 mmol), and dry dichloromethane (20.0 mL) were combined in a round bottom flask. 4-Chlorobutyrl chloride (1.20 mL, 15.0 mmol) was added and the reaction stirred at room temperature for 6 h. The solution was washed with 30.0 mL of 1 M HCl followed by 30.0 mL of saturated sodium bicarbonate solution. The organic layer was dried using anhydrous sodium sulfate, filtered, and rinsed with dichloromethane. The filtrate was evaporated to dryness and the product was purified by flash column chromatography on silica gel (30 mm × 150 mm). The column was eluted with 3:1 chloroform-hexanes and concentrated to dryness under reduced pressure. The residue was crystallized from ethyl acetate-hexanes. After cooling to room temperature the crystals were filtered and rinsed with 20.0 mL of cold 10:1 hexanes-ethyl acetate: yield = 0.47 g (9.4%); m.p. = 70 - 72 °C; R_f = 0.63 (3:1 chloroform-hexanes); ^{1}H NMR (DMSO-d_6, 600 MHz): δ 1.39 (t, *J* = 6.8 Hz, 3H), 1.54 - 1.57 (m, 2H), 1.79 −1.80 (m, 4H), 2.23 (p, *J* = 7.2 Hz, 2H), 2.65 - 2.69 (m, 2H), 2.78 (t, *J* = 6 Hz, 2H), 3.65 (t, *J* = 6 Hz, 2H), 4.33 (q, *J* = 7.2 Hz, 2H), 11.35 (s, 1H); ^{13}C NMR (DMSO-d_6, 150 MHz) δ: 14.5, 23.0, 23.1, 24.5, 26.5, 27.9, 33.6, 44.3, 60.7, 111.7, 126.9, 130.9, 147.6, 166.8, 168.8; mass spectrum (HRMS), *m/z* = 330.0910 $(M+H)^+$ $C_{15}H_{21}ClNO_3S$ requires 330.0931.

2-Chloro-*N*-(3-cyano-4,5,6,7-tetrahydrobenzo[*b*]thien-2-yl)acetamide (**2c**). Compound (**1b**) (0.500 g, 2.8 mmol) was treated with chloroacetyl chloride (0.44 mL, 5.61 mmol) in chloroform (5 mL). The reaction was refluxed for 3 h. The reaction was analyzed for completion by TLC with 9:1 hexanes – ethyl acetate. The reaction solution was concentrated under reduced pressure. The residue is crystallized from chloroform-hexanes: yield 0.418 g (59%); m.p. = 180–183 °C (Lit:[24] 171–173 °C); R_f = 0.3 (9:1 hexanes-ethylacetate); ^{1}H NMR ($CDCl_3$, 400 MHz); δ1.85 (m, 4H), 2.62 (t, *J* = 5.6 Hz, 2H), 2.66 (t, *J* = 4.4 Hz, 2H),

4.28 (s, 2H), 9.38 (s, 1H); mass spectrum (ESIMS), *m/z* = 277 $(M+Na)^+$, $C_{11}H_{11}ClN_2OS$ requires 277.

4-Chloro-*N*-(3-cyano-4,5,6,7-tetrahydrobenzo[*b*]thien-2-yl)butanamide (**2d**). Compound **1b** (1.07 g, 6.00 mmol), triethyl amine (2.50 mL, 18.0 mmol), and dry dichloromethane (20 mL) were combined in a round bottom flask. The reaction occurred under dry nitrogen and 4-chlorobutyrl chloride (2.03 mL, 18.0 mmol) was added. The reaction was analyzed for completion by TLC using 3:1 hexanes-ethyl acetate. The solution was washed with 30 mL of 1 M HCl in a separatory funnel; the organic layer was then washed with 30 mL saturated sodium bicarbonate solution. The organic layer was dried using anhydrous sodium sulfate, filtered, and rinsed with dichloromethane. The product was concentrated to dryness under reduced pressure. The product was decolorized by using carbon decolorizing charcoal in ethyl acetate solution. The solution was filtered, concentrated, and crystallized by chloroform and hexanes. Crystals were rinsed and filtered with cold 1:1 chloroform-hexanes: yield = 1.48 g (29%); m.p. = 158 - 161 °C (Lit:[54] m.p. = 186–187 °C, Lit:[55] m.p. = 143–146 °C); R_f = 0.5 (3:1 hexanes-ethyl acetate); ^{1}H NMR ($CDCl_3$, 400 MHz): δ 1.92–1.87 (m, 2H), 2.15 (p, *J* = 6.4 Hz, 2H), 2.70 (t, *J* = 5.6 Hz, 1H), 2.77 (t, *J* = 4.4 Hz, 1H), 2.89 (t, *J* = 7.2 Hz, 2H), 3.63 (t, *J* = 6.0 Hz, 2H) 9.08 (s, 1H); ^{13}C NMR ($CDCl_3$, 100 MHz): δ 22.3, 23.3, 24.1(2), 32.8, 27.9, 44.4, 92.5, 115.0, 128.2, 130.9, 147.7, 169.6; mass spectrum (ESIMS), *m/z* = 283 $(M+H)^+$ $C_{13}H_{16}ClN_2OS$ requires 283.

2-(Acetylthio)alkanamido-4,5,6,7-tetrahydrobenzo[*b*]thiophene derivatives **3a–d**. Potassium thioacetate (0.423 mg, 3.78 mmol) was added to a solution of 2-(chloroalkyl) aminothiophene derivatives **2a–d** (3.15 mmol) in anhydrous DMF (25 mL) under nitrogen. The reaction mixture was stirred overnight, and the solvent was removed under reduced pressure. The residue was dissolved in ethyl acetate (15 mL), and the resulting solution was washed with water. The combined organic extracts were dried over anhydrous Na_2SO_4, filtered and the solvent was removed under reduced pressure. The residue was purified by flash chromatography to give the acetylthio derivatives **3a–d**.

Ethyl 2-(2-(acetylthio)acetamido)-4,5,6,7-tetrahydrobenzo[*b*]thiophene-3-carboxylate (**3a**). Potassium thioacetate (43.9 mg, 0.385 mmol) was added to a conical vial containing a solution of 2-(chloroalkyl) aminothiophene derivative **2a** (100 mg, 0.332 mmol) in anhydrous DMF (5.0 mL) under nitrogen. The reaction mixture was stirred at room temperature for 20 h and diluted with ethyl acetate (10.0 mL). The resulting solution was washed with water and the combined organic extracts were dried with anhydrous sodium sulfate, filtered, and concentrated under reduced pressure. The crude product was purified by flash column chromatography on silica gel (30 mm × 150 mm) eluting with 1:4 ethyl acetate-hexanes. The solid could be crystallized from ethyl acetate-hexanes to generate yellow microcrystals: yield = 68.9 mg (62%); m.p. = 115–116 °C; R_f = 0.48 (1:4 ethyl acetate-hexanes); ^{1}H NMR ($CDCl_3$, 400 MHz): δ 1.38 (t, *J* = 7.2 Hz, 3H) 1.77 - 1.78 (m, 4H), 2.46 (s, 3H), 2.63 - 2.64 (m, 2H), 2.76 - 2.77 (m, 2 H), 3.82 (s, 2H), 4.36 (q, *J* = 6.8 Hz, 2H), 11.68 (s, 1H); ^{13}C NMR ($CDCl_3$, 150 MHz): δ 14.3, 22.8, 22.9, 24.3, 26.3, 30.2, 33.0, 60.5, 112.3, 127.1, 131.0, 146.6, 164.8, 166.2, 194.0; mass spectrum (HRMS), *m/z* = 364.0630 $(M+Na)^+$, $C_{15}H_{19}NNaO_4S_2$ requires 364.0653.

Ethyl 2-(4-(acetylthio)butanamido)-4,5,6,7-tetrahydrobenzo[*b*]thiophene-3-carboxylate (**3b**). The solid could be crystallized from ethyl acetate-hexanes to generate yellow needles: yield 0.78g (66%); m.p. = 74.0–74.5 °C; ^{1}H NMR ($CDCl_3$, 600 MHz): δ 1.38 (t, *J* = 7.2 Hz 3H), 1.78 (m, 4H), 2.03 (m, 2H), 2.33 (s, 3H), 2.54 (m, 2H), 2.63 (m, 2H), 2.76 (m, 2H), 2.97 (m, 2H), 4.37 (q, *J* = 6.8 Hz, 2H), 11.28 (s,1H); ^{13}C NMR ($CDCl_3$, 600 MHz): δ 14.3, 22.8, 22.9, 24.3, 25.0, 26.3, 28.3, 30.6, 35.2, 60.5, 111.4, 126.6, 130.6, 147.3, 166.6, 195.5; mass spectrum (HRMS), *m/z* = 392.0938 $(M+Na)^+$, $C_{17}H_{23}NNaO_4S_2$ requires 392.0966.

4-(3-Cyano-4,5,6,7-tetrahydrobenzo[*b*]thiophen-2-ylamino)-4-oxoethyl ethanethioate (**3c**). The solid could be crystallized from ethyl acetate-hexanes to generate yellow needles: yield 0.89g (96%); m.p. = 170.0–170.5 °C; ^{1}H NMR ($CDCl_3$, 600 MHz): δ 1.83 - 1.79 (m, 4H), 2.47 (s, 3H), 2.58 - 2.57 (m, 2H), 2.63 - 2.59 (m, 2H), 3.78 (s, 2H), 9.48 (s, 1H); ^{13}C NMR ($CDCl_3$, 600 MHz): δ 22.0, 23.0, 23.9, 23.9, 30.2, 32.8, 94.1, 113.9, 128.6, 131.1, 146.1, 165.1, 196.5; mass spectrum (ESIMS), *m/z* = 295 $(M+H)^+$ $C_{13}H_{15}N_2O_2S_2$ requires 295.

4-(3-Cyano-4,5,6,7-tetrahydrobenzo[*b*]thiophen-2-ylamino)-4-oxobutyl ethanethioate (**3d**). Yield 0.79g (78%); ^{1}H NMR ($CDCl_3$, 600 MHz): δ 1.85 (m, 4H), 2.03 (m, 2H), 2.33 (m, 2H), 2.34 (s, 3H), 2.55 (m, 4H), 2.95 (m, 2H), 9.40 (s, 1H); ^{13}C NMR ($CDCl_3$, 600 MHz): δ 22.8, 22.9, 24.3, 25.0, 26.3, 29.3, 32.6, 34.2, 91.5, 114.4, 128.6, 132.6, 148.3, 170.8, 196.5; mass spectrum (HRMS), *m/z* = 322.0527 $(M+Na)^+$, requires 322.0548.

Ethyl 2-[(4-bromobutanoyl)amino]-4,5,6,7-tetrahydrobenzo[*b*]thiophene-3-carboxylate (**4a**). Compound **1a** (0.600 g, 2.66 mmol) was dissolved in dichloromethane (15 mL) and cooled to 0 °C. 4-Bromobutyrl chloride (0.366 mL, 3.16 mmol) was added drop wise under nitrogen atmosphere. The reaction was stirred continuously for 1.5 h and analyzed for completion by TLC using 3:1 (hexanes-ethyl acetate). Upon completion, the reaction mixture was washed with brine (3 × 20 mL), satd $NaHCO_3$ (3 × 20 mL), and 1 N HCl (3 × 20 mL). The organic layer was dried using anhydrous sodium sulfate, filtered, and rinsed with dichloromethane. The crude product was purified by flash column chromatography on silica gel (30 mm × 150 mm) using 1:3 hexanes-ethyl acetate as the eluent. The product was concentrated to dryness and recrystallized from hot hexanes: yield = 0.392 g (39%); m.p. = 80–81 °C; R_f = 0.5 (3:1 hexanes-ethyl acetate); ^{1}H NMR ($CDCl_3$, 400 MHz): δ 1.39 (t, *J* = 6.8 Hz, 2H), 3H) 1.77–1.79 (m, 4H), 2.31 (p, *J* = 6.4 Hz, 2H), 2.62–2.67 (m, 4H), 2.69–2.77 (m, 2H), 3.52 (t, *J* = 6.4 Hz, 2H), 4.33 (p, *J* = 7.2 Hz, 2 H), 11.34 (s,1H); ^{13}C NMR ($CDCl_3$, 400 MHz) δ 14.5, 23.0, 23.1, 24.5, 26.5, 28.0, 33.0, 34.9, 60.7, 111.6, 126.9, 131.0, 147.4, 166.3, 168.7; mass spectrum (HRMS), *m/z* = 396.0253 $(M+H)^+$ $C_{15}H_{20}BrNO_3SNa$ requires 396.0245; Anal. Calcd for $C_{15}H_{20}BrNO_3S$: C, 48.13; H, 5.39; N, 3.74. Found: C, 48.78; H, 5.41; N, 3.77.

4-Bromo-*N*-(3-cyano-4,5,6,7-tetrahydrobenzo[*b*]thiophen-2-yl)butanamide (**4b**). Compound **1b** (1.00 g, 5.61 mmol) was dissolved in dichloromethane (25 mL) and cooled to 0 °C. 4-Bromobutyrl chloride (0.773 mL, 6.68 mmol) was added drop wise under nitrogen atmosphere and the reaction was stirred continuously for 1.5 h. The reaction was analyzed for completion by TLC using 3:1 hexanes-ethyl acetate. Upon completion, the reaction mixture was washed with brine (3 × 20 mL), satd $NaHCO_3$ (3 × 20 mL), and 1 N HCl (3 × 20 mL). The organic layer was dried using anhydrous sodium sulfate, filtered, and concentrated under reduced pressure. The crude product was purified by flash column chromatography on silica gel (30 mm × 150 mm) using 1:3 hexanes-ethyl acetate as the eluent. The product was concentrated to dryness and recrystallized using dichloromethane-hexanes: yield = 1.23 g (67%); m.p. = 173–174 °C; R_f = 0.5 (3:1 hexanes-ethyl acetate); ^{1}H NMR ($CDCl_3$, 600 MHz): δ 1.53–1.59 (m, 1H) 1.83–1.84 (m, 4H), 2.31 (p, *J* = 6.6 Hz, 2H), 2.60–2.64 (m, 4H), 2.69 (t, *J* = 7.2 Hz, 2H), 3.53 (t, *J* = 6.0 Hz, 2H), 8.57 (m,1H, NH); ^{13}C NMR ($CDCl_3$, 600 MHz): δ 22.3, 23.3, 24.1, 24.2, 27.9, 33.1, 34.1, 92.8, 114.9, 128.4, 131.0, 147.3, 169.2; mass spectrum (ESIMS), *m/z* = 349 $(M+Na)^+$ $C_{13}H_{15}BrN_2NaOS$ requires 349; Anal. Calcd for $C_{13}H_{15}BrN_2OS$: C, 47.71; H, 4.62; N, 8.56. Found: C, 47.82; H, 4.44; N, 8.53.

Ethyl 2-(3-(2-chloroethyl)ureido)-4,5,6,7-tetrahydrobenzo[*b*]thiophene-3-carboxylate (**5**). A solution of ethyl 2-amino-4,5,6,7-tetrahydrobenzo[*b*]thiophene-3-carboxylate **1a** (1.125 g, 5.00 mmol) in toluene (5 mL) was treated with 2-chloroethyl isocyanate (0.636 mL, 7.50 mmol). The resulting solution was refluxed at 112 °C for 3 h under dry nitrogen. The

solution was allowed to cool to room temperature and was then concentrated under reduced pressure. The crude product was purified by flash column chromatography on silica gel (75 mm × 50 mm) eluting with 1:9 ethyl acetate-hexanes. The product was concentrated to dryness and crystallized from 2:2:6 dichloromethane–diethyl ether-hexanes): yield: 867 mg (53%); R_f = 0.56 (3:7 ethyl acetate-hexanes); m.p. = 119–123°C (Lit:[56] 123–125°C); ^{1}H NMR (600 MHz, $CDCl_3$): δ 1.37–1.35 (t, J = 7.2 Hz, 3H), 1.78–1.77 (m, 4H), 2.60 - 2.58 (d, J = 6 Hz, 2H), 2.74 - 2.73 (d, J = 6 Hz, 2H), 3.68 – 3.65 (m, 4H), 4.31 - 4.27 (q, J = 7.2, Hz, 2H), 5.52 (s, 1H); ^{13}C NMR (600 MHz, $CDCl_3$): δ 14.4, 23.0, 24.4, 26.5, 42.5, 44.2, 60.4, 77.2, 109.4, 125.1, 130.6, 150.8, 153.7, 167.1; mass spectrum (ESIMS), m/z = 332 $(M+H)^+$, $C_{14}H_{20}ClN_2O_3S$ requires 332.

Methyl 5-*O*-*p*-Toluenesulfonyl-α-D-arabinofuranoside (**6**).[24] Methyl α-D-arabinofuranoside[24] (3.05 mmol) was dissolved in 20 mL of pyridine. Tosyl chloride was then added in slight excess (3.25 mmol) and the solution stirred at 37 °C for 24 hours under dry nitrogen. The heat was removed and the reaction was allowed to progress at room temperature for an additional 5 days. Ice was used to quench the reaction and an additional 60 mL of water was added along with 15 mL of brine. The solution was extracted with ethyl acetate (3 × 35 mL). The organic layers were combined and back extracted with water and brine. Anhydrous sodium sulfate was used to dry the solution which was then filtered and concentrated. The crude product was purified by flash column chromatography on silica gel (50 mm × 150 mm) eluting with 3:3:14 acetone-chloroform-hexanes (500 mL), followed by 1:1:3 acetone-chloroform-hexanes (250 mL), and finally followed by 1:1:2 acetone-chloroform-hexanes (200 mL). The product fractions were pooled and concentrated: yield 633 mg (65%); R_f = 0.45 (1:9 methanol-chloroform).

Methyl 5-*O*-*p*-Toluenesulfonyl-2,3-di-*O*-Acetyl-α-D-arabinofuranoside (**7**).[57,58] Compound **7** (1.28 g, 3.88 mmol) was dissolved in 30 mL of 1:1 pyridine-acetic anhydride in a round bottom flask. The solution was allowed to stir at room temperature under dry nitrogen for 24 h. The reaction was quenched with ice (30.0 g) and extracted using dichloromethane and back extracted with brine. The solution was dried with anhydrous sodium sulfate, filtered, and concentrated under reduced pressure. The crude product was purified by flash column chromatography on silica gel (30 mm × 150 mm). The product was eluted with 1:3 ethyl acetate-hexanes, followed by 1:1 ethyl acetate-hexanes (100 mL). The product fractions were pooled and concentrated under reduced pressure: yield 1.15 g (73%); R_f = 0.16 (1:3 ethyl acetate-hexanes); ^{1}H NMR ($CDCl_3$, 600 MHz): δ 2.08 (s, 6H), 2.45 (s, 3H), 3.36 (s, 3H), 4.16 - 4.18 (m, 1H), 4.26 (dd, 1H, J = 5.4, 10.8 Hz), 4.32 (dd, 1H, J = 3, 10.8 Hz), 4.87 (m, 1H), 4.89 (s, 1H), 5.02 (s, 1H), 7.35 (d, 2H, 6.6 Hz), 7.81 (d, 1H, J = 6.6 Hz); ^{13}C NMR (600 MHz, $CDCl_3$): δ 20.9, 21.9, 55.6, 68.9, 71.4, 75.9, 78.8, 80.7, 81.1, 81.1, 107.0, 128.1, 128.2, 128.3, 130.1, 130.1, 133.0, 145.2, 170.1, 170.5, 170.7.

Methyl 2,3-tri-*O*-acetyl-5-*S*-acetyl-5-thio-α-D-arabinofuranoside (**8**).[21] Compound **7** (1.15 g, 2.86 mmol) was dissolved in 10 mL of anhydrous DMF in a round bottom flask. An additional 10 mL of anhydrous DMF was used to dissolve $KSCOCH_3$ (0.40 g, 3.50 mmol). The $KSCOCH_3$ solution was then added dropwise to the starting material and allowed to stir at room temperature under nitrogen for 24 h. The solution was diluted with 50 mL of water and extracted with three 30 mL-portions of ether. The ether layers were combined and washed with saturated sodium chloride solution. The ether was dried with anhydrous sodium sulfate, filtered, and concentrated under reduced pressure. The crude product was purified by flash column chromatography on silica gel (30 mm × 150 mm). The product was eluted with 1:1:5 acetone-chloroform-hexanes and concentrated to dryness under reduced pressure: yield = 525 mg (60%); R_f = 0.39 (2:3 ethyl acetate-hexanes); ^{1}H NMR ($CDCl_3$, 600 MHz): δ 2.03 (s, 6H), 2.33 (s, 3H), 3.12 - 3.17 (m, 1H), 3.32–3.37 (m, 4H), 4.14 (dd, 1H, J = 5.2, 12 Hz), 4.84 (s, 1H), 4.86 (d, 1H, J = 6.0), 4.98 (s, 1H). ^{13}C NMR (600 MHz, $CDCl_3$): 21.0, 30.7,

31.3, 55.2, 78.2, 79.7, 81.9, 106.8, 170.0, 170.3, 194.9; mass spectrum (HRMS), *m/z* = 329.0646 $(M+Na)^+$, $C_{12}H_{18}NaO_7S$ requires 329.0671.

Methyl α-D-arabinofuranoside-5-thiol (**9**). A solution of 8 (3.37 g, 11.0 mmol) in 0.1 M methanolic NaOMe (40 mL) was stirred for 4 hours at 50 °C under nitrogen and neutralized with Amberlite IR120 (H+ form). The resin was filtered off, and the filtrate was concentrated under reduced pressure. The residue was extracted with ethyl acetate to provide thiol **9** after concentration: yield 1.21 g (61%); ^{1}H NMR ($CDCl_3$, 600 MHz): δ 1.68 - 1.65 (t, ^{1}H *J* = 6.0 Hz), 2.81 - 2.77 (m, 1H), 2.89 - 2.81 (m, 1H), 3.39 (s, 3H), 3.92 - 3.91 (m, 2H), 4.09 - 4.06 (m, 3H), 4.85 (s, 1H); ^{13}C NMR ($CDCl_3$, 600 MHz): δ 26.9, 55.8, 79.9, 81.7, 84.4, 108.3; mass spectrum (HRMS), *m/z* = 203.0337 $(M+Na)^+$, $C_6H_{12}NaO_4S$ requires 203.0354.

5-Iodo-α-D-arabinofuranoside (**11**). Methyl α-D-arabinofuranoside (**10**) (1.00 g, 6.66 mmol) was dissolved in dry THF (10 mL) and placed on ice. The reaction was cool to 0 °C in an ice bath and imidazole (1.07 g, 15.8 mmol), iodine (2.01 g, 7.92 mmol), and triphenylphosphine (2.00 g, 7.92 mmol) were added. The solution was warmed to 65 °C and allowed to stir for 1.5 h. The solution was diluted with 50 mL of water and extracted with dichloromethane (3 × 30 mL). The organic layers were combined, dried with anhydrous sodium sulfate, filtered, and concentrated under reduced pressure. The crude product was purified by flash column chromatography on silica gel (30 mm × 150 mm). The product was eluted with 8:1 chloroform-acetone and concentrated to dryness under reduced pressure: yield = 1.13 g (65%); R_f = 0.50 (3:1 chloroformacetone); ^{1}H NMR (DMSO, 400 MHz) δ 3.25 (s, 2H), 3.35 (s, 3H), 3.46–3.59 (m, 2H), 3.83 (s, 1H), 4.64 (s, 1H), 5.39–5.40 (m,1H), 5.49–5.50 (m,1H); ^{13}C NMR (DMSO, 100 MHz) δ 09.1, 54.5, 80.6, 81.2, 82.0, 108.8; mass spectrum (ESIMS), *m/z* =297 $(M+Na)^+$. Anal. Calcd for $C_6H_{11}IO_4$: C, 26.30; H, 4.05; N, 0.00; Found: C, 26.04; H, 4.02; N, 0.03.

Ethyl 2-(methyl 5-thio-α-D-arabinofuranoside-5-*S*-yl)acetamido-4,5,6,7-tetrahydrobenzo[*b*]thiophene-3-carboxylate (**13a**). Step 1: Compound (**2a**) (0.100 g, 0.33 mmol) and thiourea (0.504 g, 0.66 mmol) was suspended in 2 mL of absolute ethanol and stirred for 3 h at 65 °C. The reaction was analyzed for completion by TLC 3:1 hexanes-ethylacetate. The reaction was cooled and filtered. The filtrate was rinsed with absolute ethanol and concentrated to dryness under reduced pressure. Compound **12a** was obtained as yellow color residue: yield 0.100 g (80%); mass spectrum (ESIMS), *m/z* = 342 $(M)^+$, $C_{14}H_{20}N_3O_3S_2^+$ requires 342. Step 2: Compound (**12a**) (0.100 g, 0.29 mmol) was combined with compound **11** (0.040 g, 0.14 mmol), cesium carbonate (0.19 g, 0.584 mmol) in dry DMF (2 mL). The solution was stirred for 16 h at 85 °C under nitrogen atmosphere. The reaction was monitored by using TLC (2:1 toulene-acetone). On completion, the crude reaction mixture was loaded onto silica gel and the residual solvent evaporated under reduced pressure. The sample was loaded on silica gel column (30 mm × 150 mm) and eluted with hexanes followed by 4:1 toluene-acetone to afford the product. The product fractions were combined, concentrated under reduced pressure. The product was pink amorphous solid: yield 0.018 g (28%); R_f = 0.37 (2:1 toulene – acetone); ^{1}H NMR ($CDCl_3$, 600 MHz); δ 1.39 (t, *J* = 7.2 Hz, 3H), 1.79 (m, 4H), 2.65 (m, 2H), 2.76 (m, 2H), 2.98 (m, 2H), 3.36 (s, OCH_3), 3.53 (d, *J* = 16.2 Hz, 1H), 3.64 (d, *J* = 16.2 Hz, 1H), 3.98 (m, 1H), 4.0 (m, 1H), 4.23 (m, 1H), 4.34 (q, *J* = 7.2 Hz, 2H), 4.89 (s, 1H). ^{13}C NMR (CD_3OD, 400 MHz); δ 12.4, 20.2, 20.4, 20.6, 30.4, 30.6, 50.4, 60.0, 80.0, 80.2, 80.3, 100.9, 112.0, 126.0, 129.0, 146.0, 165.0,167.0; mass spectrum (HRMS), *m/z* = 468.1089 $(M+Na)^+$, $C_{19}H_{27}NNaO_7S_2$ requires 468.1127.

N-(3-cyano-4,5,6,7-tetrahydrobenzo[*b*]thiophen-2-yl)-2-(methyl 5-thio-α-D-arabinofuranoside-5-*S*-yl)acetamide (**13b**). Step 1: Compound (**2c**) (0.200 g, 0.78 mmol)

and thiourea (0.119 g, 1.57mmol) were suspended in 4 mL absolute ethanol and stirred for 3 h at 65 °C. The reaction was analyzed for completion by TLC using 3:1 hexanes – ethyl acetate. The reaction was cooled and filtered. The filtrate was rinsed with a minimal amount of absolute ethanol and concentrated to dryness under reduced pressure. Compound **12b** was obtained as brown color residue: yield 0.216 g (83%); mass spectrum (ESIMS), *m/z* = 295 $(M)^+$, $C_{12}H_{15}N_4OS_2^+$ requires 295. Step 2: Compound 12b (0.118 g, 0.36 mmol) was combined with Compound 11 (0.05mg, 0.18mmol), Cesium carbonate (0.234 g, 0.72 mmol) in dry DMF (2 mL). The solution was stirred for 16 h at 85 °C under nitrogen atmosphere. The reaction was monitored in thin layer chromatography using (2:1 toluene-acetone). On completion, the crude reaction mixture was loaded onto silica gel and the residual solvent evaporated under reduced pressure. The sample was loaded on silica gel column (30 mm × 150 mm) and eluted with hexanes followed by 4:1 toluene-acetone to afford the product. The product was orange amorphous solid: yield 0.040 g (56%); R_f = 0.39 (2:1 toulene – acetone); m.p. = 160–163 °C. ^{1}H NMR (CD_3OD, 600 MHz); δ 1.8 (m, 4H), 2.51 (m, 2H), 2.59 (m, 2H), 2.85 (dd, *J* = 24.6 Hz, 7.2 Hz, 1H), 2.93 (dd, *J* = 18.6 Hz, 4.2 Hz, 1H), 3.26 (s, OCH_3), 3.52 (d, *J* = 15 Hz, 1H), 3.54 (d, *J* = 15 Hz, 1H), 3.76 (m, 1H), 3.86 (m, 1H), 3.98 (m, 1H), 4.68 (d, *J* =1.8 Hz, 1H). ^{13}C NMR (CD_3OD, 400 MHz); δ 23.4, 24.3, 24.9, 25.1, 35.9, 36.5, 55.4, 81.7, 83.6, 84.5, 110.5, 114.9, 129.9, 132.6, 169.9; mass spectrum (HRMS), *m/z* = 421.0873 $(M+Na)^+$, $C_{17}H_{22}N_2O_5S_2$ requires 421.0868.

Ethyl 2-(methyl 5-thio-α-D-arabinofuranoside-5-*S*-yl)butamido-4,5,6,7-tetrahydrobenzo[*b*]thiophene-3-carboxylate (**13c**). Step 1: Compound **4a** (0.275 g, 0.725 mmol) and thiourea (0.110 g, 1.45 mmol) were suspended in 2 mL of absolute ethanol and stirred at reflux for 4 h. The reaction was analyzed for completion by TLC using 3:1 hexanes-ethyl acetate. The reaction was cooled on ice and filtered. The filtrate was rinsed with a minimal amount of absolute ethanol and concentrated to dryness under reduced pressure. Compound **12c** was obtained as colorless crystals. yield = 0.170 g (52%); m.p. = 212–213 °C; ^{1}H NMR (DMSO, 400 MHz) δ 1.25 (t, *J* = 7.2 Hz, 3H), 1.63 (br. s, 4H), 1.85–1.92 (m, 2H), 2.59–2.62 (m, 4H), 3.18 (t, *J* = 7.2 Hz, 2H), 3.37–3.41 (m, 1H), 4.22 (p, *J* = 6.8 Hz, 2H), 9.00–9.11 (m, 4H), 10.95 (s, 1H); ^{13}C NMR (DMSO, 400 MHz) δ 14.1, 22.3, 22.5, 23.7, 24.3, 25.8, 29.4, 34.1, 60.3, 111.2, 125.9, 130.3, 145.9, 165.0, 168.9, 169.7; Anal. Calcd for $C_{16}H_{24}BrN_3O_3S_2$: C, 42.67; H, 5.37; N, 9.33;. Found: C, 42.46; H, 5.17; N, 9.34. Step 2: Compound **12c** was combined with compound **11** (0.110 g, 0.244 mmol) and cesium carbonate (0.268 g, 0.825 mmol) in dry DMF (4 mL). The solution was stirred for 16 h at 85 °C under nitrogen atmosphere. The reaction was monitored by TLC using (2:1 toluene/acetone). Upon completion, the crude reaction mixture was loaded onto silica gel and DMF was evaporated under reduced pressure. The dry slurry was purified by flash column chromatography on a silica gel (30 mm × 150 mm). Elution with 4:1 toluene-acetone affords a partially purified product. The compound was further purified on a second silica gel column to remove residual DMF, eluting with (4:1 ethyl acetate/hexanes). The product fractions were combined, concentrated, and dried in vacuum where the product crystallized upon standing: yield = 0.080 g (77%); R_f = 0.53 (2:1 toulene – acetone); m.p. = 92–93 °C; ^{1}H NMR ($CDCl_3$, 400 MHz) δ 1.39 (t, *J* = 6.8 Hz, 3H), 1.78–1.79 (m, 4H), 2.04 (t, *J* = 7.2 Hz, 3H), 2.59–2.64 (m, 2H), 2.70–2.77 (m, 3H), 2.83–2.90 (m, 2H), 3.38 (s,3H), 3.90–3.93 (m,1H), 4.06 (d, *J* = 6.8 Hz, 1H), 4.20–4.22 (m, 1H), 4.34 (q, *J* = 7.2 Hz, 2H), 4.90 (s, 1H), 5.39 (d, *J* = 6.0 Hz, 1H), 11.32 (s, 1H) ppm; ^{13}C NMR ($CDCl_3$, 400 MHz) δ 14.5, 23.0, 23.2, 24.5, 25.0, 26.6, 32.8, 34.5, 55.1, 60.8, 80.5, 80.7, 85.7, 109.1, 111.7, 127.0, 131.0, 147.5, 167.0, 169.4 ppm; mass spectrum (ESIMS), *m/z* = 496.2 $(M+Na)^+$ Anal. Calcd for $C_{21}H_{31}NO_7S_2$: C, 53.26; H, 6.60; N, 2.96; O, 23.65; S, 13.54. Found: C, 53.32; H, 6.51; N, 2.93.

N-(3-cyano-4,5,6,7-tetrahydrobenzo[*b*]thiophen-2-yl)-2-(methyl-5-thio-α-D-arabinofuranoside-5-*S*-yl)butamide (**13d**). Step 1: Compound **4b** (0.300 g, 0.916 mmol) and

thiourea (0.139g, 1.83 mmol) was suspended in 2 ml of absolute EtOH was stirred at reflux for 4h. The reaction was analyzed for completion by using TLC 3:1 (Hexanes/Ethyl Acetate). The reaction mixture was cooled on ice and filtered with minimal amount of abs EtOH and dried in vacco. Compound **12d** was obtained in colorless crystals: yield = 0.262 g (71%); m.p. = 205–207 °C ^{1}H NMR (DMSO, 600 MHz) δ 1.67 (m, 4H), 1.83–1.85 (m, 3H), 2.01 (s, 2H), 2.40–2.44 (m, 2H), 2.55-2.58(m, 2H), 3.12–3.132 (m, 2H), 8.98 (m,1H) ppm; ^{13}C NMR (DMSO, 600 MHz) δ 21.7, 22.6, 23.3, 23.5, 24.0, 29.5, 30.7, 33.1, 114.3, 127.1, 130.6, 146.4, 169.6, 170.1 ppm; Anal. Calcd for $C_{14}H_{19}BrN_4OS_2$: C, 41.69; H, 4.75; Br, 19.81; N, 13.89; O, 3.97; S, 15.90. Found: C, 40.88; H, 4.57; N, 14.20. Step 2: Compound **12d** was combined to compound **11** (0.210g, .520 mmol), cesium carbonate (0.268g, 0.825 mmol) were dissolved in dry DMF (5 ml). The solution was stirred for 24 h at 85 °C under nitrogen atmosphere. The reaction was monitored by thin layer chromatography using (1:1 acetone-hexanes). Upon completion, the crude reaction mixture was loaded onto silica gel and the DMF was evaporated under reduced pressure. The dry slurry was purified by flash column chromatography on a silica gel (30 mm × 150 mm). Elution was with 2:1 acetone-hexanes. The product fractions were combined and concentrated to dryness. The crude product was crystallized using ethanol and filtered with cold ethanol: yield = 0.110 g (49%); R_f = 0.3 (1:1 acetone - hexanes); m.p. = 183–184 °C; ^{1}H NMR (DMSO, 600 MHz) δ 1.69 (s, 4H), 1.80 (p, J = 6.0 Hz, 4H), 2.42 (br. s, 2H), 2.51–2.62 (m, 4H), 2.73 (s, 1H), 3.18 (s,3H), 3.56–3.58 (m,1H), 3.71–3.72 (m, 1H), 3.74–3.76 (m, 1H), 4.55 (s, 1H), 5.25 (d, J = 6, 1H), 5.39 (d, J = 6.0 Hz, 1H), 11.51 (br. s, 1H) ppm; ^{13}C NMR (DMSO, 400 MHz) δ 21.8, 22.7, 23.3, 23.5, 24.8, 31.6, 33.8, 33.9, 54.4, 79.9, 80.1, 81.9, 82.6, 92.2, 109.0, 114.4, 127.04, 130.6, 146.67, 170.66 ppm; mass spectrum (HRMS), m/z = 449.1199 $(M+Na)^+$ $C_{19}H_{26}N_2O_5S_2Na$ requires 449.1181; Anal. Calcd for $C_{19}H_{26}N_2O_5S_2$: C, 53.50; H, 6.14; N, 6.57; O, 18.75; S, 15.03. Found: C, 48.78; H, 5.41; N, 3.71.

Methyl 5-*S*-[2-(2,4-dioxo-1,4,5,6,7,8-hexahydro[1]benzothieno[2,3-d]-pyrimidin-3(2*H*)-yl)ethyl]-5-thioarabinofuranoside (**14**). Compound **10** (0.194 g, 0.634 mmol) and compound **5** (0.289 g, 0.868 mmol) were combined in 3 mL NaOMe (3.06 mmol Na metal in 3 mL NaOH). The solution was stirred at room temperature for 24 h then was quenched using 20 mL 1N HCl. The solution was diluted with water and extracted with chloroform (3 × 20mL). The chloroform was dried with anhydrous sodium sulfate, filtered, and dried under reduced pressure. The product was purified by flash column chromatography on silica gel (30 mm × 150 mm) eluting with 50:50 hexanes-acetone. The product fractions were concentrated to afford **14**, a colorless waxy solid: yield = 36 mg (13%); R_f = 0.46 (1:1 hexanes – acetone); ^{1}H NMR ($CDCl_3$, 600 MHz): δ 1.78 (m, 4H), 2.60 (s, 2H), 2.83 - 3.04 (m, 6H), 3.37 (s, 3H), 4.03 (br. s, 2H), 4.13 (br. s, 1H), 4.19 (m, 4H), 4.88 (s, 1H), 10.91 (br. s, 1H); ^{13}C NMR ($CDCl_3$, 600 MHz): δ 22.2, 23.2, 24.7, 25.5, 30.3, 34.3, 39.8, 55.4, 80.0, 81.5, 83.9, 108.8, 114.0, 127.3, 132.2, 148.7, 152.2, 159.1; mass spectrum (HRMS), m/z = 451.0969 $(M+Na)^+$, $C_{18}H_{25}N_2O_6S_2$ requires 429.1154.

Results and Discussion

Molecular Modeling

The substrate analogues shown in Figure 2 all contain the 2-amino-4,5,6,7-tetrahydrobenzo[*b*]thiophene scaffold. Different linker lengths and the arabinose moiety were converted to 3-dimensional structures (MDL mol file format) using Chem3D (CambridgeSoft). The compound data sets were then imported into Maestro V8.0 (Schrodinger, Inc) and were prepared for docking using MacroModel (Schrodinger, Inc) by using conformational analysis and minimization methods to obtain the lowest energy conformer. The crystallographic coordinates for the Ag85C-octylthioglucoside complex

(PDB code: 1va5)[29] was obtained from the Protein Data Bank (www.rcsb.org) and prepared by removing all the solvent and adding hydrogen atoms and minimal minimization in the presence of bound ligand using protein preparation. Grids for molecular docking with Glide™ V4.5 (Schrodinger, Inc) were calculated without any constraint to the protein.[59] Compounds were docked using Glide™ in extra-precision mode, with up to five poses saved per molecule. The docked poses were then minimized using the local optimization feature in MacroModel,[60] and the energies were calculated using the OPLS force field[61] and the GBSA continuum model[62] in Maestro. The binding free energy ΔG_{bind} is estimated as:

$$\Delta G_{bind} = \Delta E_{MM} + \Delta G_{solv} + \Delta GSA$$

Where ΔE_{MM} is the difference in energy between the complex structure and the sum of the energies of the ligand and the unliganded protein, using the OPLS force field, ΔG_{solv} is the difference in the GBSA solvation energy of the complex and the sum of the solvation energies for the ligand and unliganded protein, and ΔG_{SA} is the difference in the surface area energy for the complex and the sum of the surface area energies for the ligand and uncomplexed protein. Corrections for entropic changes were not applied. Finally, according to the docking score and binding energy we selected the candidate structures for preparing and testing as inhibitors for Ag85C. Structures with good docking scores included compounds containing a 2-amino-4,5,6,7-tetrahydro-1-benzothiophene-3-carbonitrile or an ethyl 2-amino-4,5,6,7-tetrahydro-3-carboxylate linked through the 2-amino moiety to a methyl 5-thio-α-D-arabinofuranoside. The best docking scores are shown in Table 1 and include **13a–d** and compound **14**. Of these compounds **13a** showed the highest binding energy of −62 kJ/mol.

Potential intermolecular hydrogen bonded interactions between compound **13a** and the Ag85C protein showed four hydrogen bonds (OH-3 of the arabinose with NH of Arg41 and HOH 2037, OH-4 of the arabinose with NH of Trp262, and S of the linker with HOH 2242), Figure 3. In addition the calculated distance between the OH of Ser124 and the carbon of carbonyl carbon of the ester and were found to be separated by 6.876 Å. Finally, we calculated the electrostatic interactions between compound **13a** and the Ag85C protein, Figure 4. According to the hydrogen bond and electrostatic interactions, compound **13a** was expected to be a good template for occupying the active site of the enzyme.

Synthesis of Glycoconjugates

Both the 2-amino-4,5,6,7-tetrahydro-1-benzothiophene-3-carbonitrile and ethyl 2-amino-4,5,6,7-tetrahydro-1-benzothiophene-3-carboxylate classes of thiophenes could be accessed through a classic Gewald synthesis[52] followed by amine functionalization with an appropriate linker. The Gewald synthesis was performed by treating cyclohexanone with malononitrile or ethyl cyanoacetate and sulfur in the presence of *N*-ethylmorpholine to yield 3-carboxylate thiophene **1a** [51] and 3-carbonitrile thiophene **1b**, respectively, in a modest yield. Thiophenes **1a** and **1b** were then reacted with either chloroacetyl chloride or 4-chlorobutyrl chloride to prepare amides **2a–d**, Scheme 1, in modest yield. Alternatively, **1a** was reacted with 2-chloroethyl isocyanate to form urea **5**[56] in 53% yield. With key intermediates in hand, we explored different approaches to form a thioether linkage between the thiophenes and the C-5 position of a methyl α-D-arabinofuranoside. In the first approach, the chloro substituent of thiophenes **2a–d** was displaced with potassium thioacetate in anhydrous DMF to afford the thioesters **3a–d** in yields of 62–92%. The resulting thiophenes were treated with NaOEt, concentrated and directly reacted with the known methyl 5-*O*-*p*-toluenesulfonyl-α-D-arabinofuranoside (**6**), Scheme 3.[24,25,26] Unfortunately, we failed to isolate an identifiable product using this protocol. We then chose

to reverse the polarity of the electrophile by converting the tosylate to a sulfhydryl. This required peracetylation of arabinofuranoside **6** with acetic anhydride to afford the diacetylated compound **7** in 73% yield, Scheme 2. Acetylated sulfonate **7** was then treated with potassium thioacetate to afford the thioester **8** in 60% yield. Arabinofuranoside **8** was then treated with NaOMe at 50 °C for 2 h. The reaction was neutralized with Amberlite IR120 (H+ form), filtered and dried. The resulting methyl 5-deoxy-5-thio-α-D-arabinofuranoside **9** was resuspended in THF and combined with an equivalent of alkyl chlorides **2a–d** and triethyl amine to afford glycoconjugates **13a–d**, Scheme 3. In our hands, only the α-chloroamides **2a** and **2c** reacted with the mercaptan **9** to produce thioethers **13a** and **13b**, respectively, in unacceptable yield. Modification of bases, solvents and addition of disulfide reducing agents failed to generate the longer chain thioethers.

Unsatisfied with failure of the reaction between halides **2b** and **2d** and mecaptan **9**, as well as poor coupling yields to this point, we began to explore alternate options for synthesizing the desired thioether linkages. There are numerous examples of alkyl halides reacting with isothiourionium salts to form thioethers.[63] Therefore, we converted methyl α-D-arabinofuranoside (**10**)[24,25,26] to the known methyl 5-deoxy-5-iodo-α-D-arabinofuranoside (**11**) using I_2-$P(Ph)_3$-imidizole in 65 % yield (Scheme 2).[64] Compounds **1a** and **1b** were then acylated with 4-bromobutyrl chloride to provide amides **4a** and **4b**, respectively (Scheme 1). Amides **2a**, **2c**, **4a** and **4b** were then treated with thiourea in refluxing ethanol to afford the respective isothiourionium salts **12a–d**, in good yield (Scheme 3). The isothiourionium salts reacted cleanly with iodide **11** in the presence of cesium carbonate in *N,N*-dimethylformamide to form thioethers **13a–d**, respectively.

We also found it noteworthy that chloride **5** and methyl 5-thio-α-D-arabinofuranoside **8** in methanol-NaOMe, afforded the 3-substituted pyrimidinedione **14** linked to a methyl 5-thio-α-D-arabinofuranoside moiety (Scheme 4). There resulting materials were then used to evaluate the structural class as inhibitors of the Ag85C acyltransferase activity.

Enzyme Inhibition Studies

To determine if any compounds from this library inhibit the Ag85C enzyme, assays measuring the enzymatic activity were performed. These assays employed 4-methylumbelliferyl butyrate (4MUB) as the acyl donor and trehalose as the acyl acceptor. Binding of 4MUB within the enzyme active site allows nucleophilic attack on the substrate to produce an acyl-Ag85C intermediate and release of the fluorescent molecule 4-methylumbelliferone (4-MU). Subsequent binding of trehalose in the active site allows nucleophilic attack by trehalose on the acyl-Ag85C intermediate to form trehalose-6-butyrate. Measuring the fluorescence emission of 4-MU at 500 nm affords an accurate determination of the initial rate of the enzymatic reaction.

To determine the K_i values for the library of inhibitors, the initial reaction rate using this fluorescence-based assay was performed in the presence of varying concentrations of each inhibitor. The ratio of the rates of the inhibited reaction versus the uninhibited reaction plotted as a function of inhibitor concentration exhibits a clear dose-dependent decrease in enzymatic activity. Fitting these data allowed the calculation of K_i values for each of the inhibitors, which ranged from 18.2 to 71.0 μM, Table 1 and Figure 5A.

While the K_i values of the inhibitors do not vary significantly, a general trend is observed that offers insight for the design of second-generation compounds with improved affinity for the Ag85C enzyme and better inhibitory activity. Because of the choices of arabinofuranosides tested, the importance of two structural variables can be related to inhibitory activity. First, of the thiophene containing compounds, those elaborated with the ethylester moiety on the thiophene have slightly better inhibitory activity than compounds

with a corresponding nitrile moiety as seen when comparing the K_i values of **13a** and **13b**. Second, the length of the linker between the thioether and the aromatic fused ring system affects inhibitory activity. Compound **13a**, which contains a methylene linker, exhibits stronger inhibition than **13c**, which possesses a propylene linker. The single three-ringed compound tested is difficult to analyze in isolation. The K_i is near the middle of the range observed in the inhibition studies. Synthesis of similar compounds and further testing will be required to determine if there is a benefit to having the third ring. The compounds were screened for growth inhibition activity against *M. smegmatis*; however, no growth inhibition was observed.

Crystal Structure of the Ag85C-Inhibitor Complex

To gain insight into the mechanism of inhibition and information necessary to develop better inhibitors, specific structural information is needed. To this end, the coordinates were obtained of crystals of recombinant Ag85C soaked with compound **13a**. Compound **13a** was chosen because it possesses the lowest K_i value. Difference map calculated with these data show 4 strong regions of electron density within the Ag85C active site. These are consistent with one compound of **13a**, a single water molecule and two molecules of glycerol. The binding of **13a** within the active site indicates that it functions as a competitive inhibitor of Ag85C (Figure 5B).

The orientation of **13a** within the active site of the crystal structure (Figure 6) is different with respect to the predicted structure from the inhibitor modeling data. The thiophene moiety is positioned in roughly the same location, but is flipped 180° along the major axis of the 2 ringed system to position the ethylester pointing away from the enzyme rather than into the hydrophobic tunnel. The arabinofuranoside moiety binds within the known carbohydrate-binding site as exhibited for the Ag85B-trehalose crystal structure.[30] However, the arabinosyl moiety of **13a** overlaps with the glucosyl moiety of trehalose that is distal to Ser124 of Ag85B rather than binding in the proximal carbohydrate binding pocket that accommodates the sugar to be acylated by the enzyme.

Unexpectedly, no specific hydrogen bonding interactions are being formed between the arabinofuranoside and the carbohydrate-binding site of the active site. This would suggest that the binding is driven by hydrophobic interactions between the thiophene moiety and the mycolyl binding site, and that linker length as well as shape complementarity between the arabinosyl moiety and the carbohydrate binding site ultimately determine the location of the arabinosyl binding. The interaction between Ag85C and the arabinofuranosyl moiety is rather dissimilar to the interactions observed in the Ag85B-trehalose crystal structure, where O2 and O3 of the distal glucosyl moiety of trehalose are hydrogen bonded to the side chain of Arg41 and O6 is hydrogen bonded to the backbone carbonyl of His260.[30]

The fused, two-ring system of **13a** is positioned in the proposed mycolic acid-binding pocket and forms van der Waals interactions with the side chains of Phe150, Trp158 Leu161, Ala165 and Leu227.[29,33] In addition, the linker connecting the thiophene to the arabinofuranosides moiety forms van der Waals interactions with the side chain of Arg41. The carbonyl oxygen of the amide moiety appears to be poised to form a hydrogen bond with the backbone amide of Leu40 although the 4.5 Å distance between these is too long for a *bona fide* hydrogen bond. The approach of **13a** to the oxyanion hole is blocked by an ordered water molecule that forms hydrogen bonds with both the oxyanion hole and the amide carbonyl of **13a**. One key to improving binding and inhibitory activity of a second-generation inhibitor would be to displace this water molecule with a hydrogen bond acceptor to promote a direct interaction between the inhibitor and the oxyanion hole.

Another important piece of information from this structure can be used for future design efforts to improve both strength and specificity of binding. The pocket initially assumed to be important for binding the trehalose still has an undefined role.[33] To date, no structure has revealed binding of any substrate or product analogs within this site even though the residues forming this site (Asp38, Asp45, and Trp262) are conserved in all Ag85 complex mycolyltransferases. The only compounds observed in any structures within this site are glycerol and water, which implies that it may accommodate additional carbohydrate moieties exposed on the surface of the mycobacterial outer membrane.[28,29,33] One potential substrate accommodated by this conserved site would be a neighboring subunit of the arabinan. As the conserved sequence and structure in this region implies an important role, the Ag85C-**13a** complex structure gives very specific information regarding the future design of inhibitors that could bind within this site. Specifically, the methyl group on the methyl-arabinofuranoside can be replaced with a much bulkier moiety such as another arabinofuranosyl moiety, capable of forming a complex hydrogen bonded network with the conserved residues in this site. Alternatives other than carbohydrates could also be used. Ideally, these groups would possess a large number of both hydrogen bond donors and acceptors to maximize the interaction potential within this site.

Conclusion

Virtual thiophene-arbinoside conjugates were docked to antigen Ag85C using Glide. Compounds with good docking scores were synthesized by a Gewald synthesis followed by linking to 5-thioarabinofuranosides. The resulting thiophenyl-thioarabinofuranosides were assayed for inhibition of mycoyltransferase activity using a 4-methylumbelliferyl butyrate fluorescence assay. The conjugates showed K_i values that ranged from 18.2 to 71.0 μM. The inhibitor with the lowest K_i value, **13a**, was used to obtain a crystal structure of the inhibitor bound within the active site of Ag85C. Closely related thiophene derivatives have recently been shown to inhibit the synthesis of TDM, a mycobacterial virulence factor, and inhibit the growth of *M. tuberculosis* particularly in macrophages. The limited set of structures we identified showed no activity against *M. smegmatis*, a model organism, in a disk diffusion assay; however, the structures we identified are very similar to thiophenes which show activity in macrophages infected with drug resistant strains *M. tuberculosis*. Based on this observation, we plan to evaluate these compounds and others in a macrophage infection model. The crystal structure highlights interactions between both the thiophene and arabinofuranosides moieties and will be leveraged to design improved inhibitors of Ag85s.

Supplementary Material

Refer to Web version on PubMed Central for supplementary material.

Acknowledgments

Use of the Advanced Photon Source was supported by the U. S. Department of Energy, Office of Science, Office of Basic Energy Sciences, under Contract No. DE-AC02-06CH11357. Use of the LS-CAT Sector 21 was supported by the Michigan Economic Development Corporation and the Michigan Technology Tri-Corridor for the support of this research program (Grant 085P1000817). This was supported by an NIH grants to D.R. Ronning (AI089653) and S.J. Sucheck (GM094734). We also thank students Shen Zhang and Shuangqianzi Li for assistance with the resynthesis and characterization of key intermediates.

References

1. Institute of Medicine of the National Academies. Addressing the Threat of Drug-Resistant Tuberculosis: A Realistic Assessment of the Challenge. Washington, DC: Workshop Summary The National Academies Press; 2009.

2. Zhang Y, Amzel LM. Tuberculosis drug targets. Curr. Drug Targets. 2002; 3:131–154. [PubMed: 11958297]
3. Chatterjee, D.; Brennan, PJ. Microbial Glycobiology. In: Moran, AP., editor. Glycosylated Components of the Mycobacterial Cell Wall: Structure and Function. London: Elsevier; 2009. p. 147-167.
4. Brennan PJ, Nikaido H. The envelope of mycobacteria. Annu. Rev. Biochem. 1995; 64:29–63. [PubMed: 7574484]
5. Belanger AE, Besra GS, Ford ME, Mikusova K, Belisle JT, Brennan PJ, Inamine JM. The *embAB* genes of *Mycobacterium avium* encode an arabinosyl transferase involved in cell wall arabinan biosynthesis that is the target for the antimycobacterial drug ethambutol. Proc. Natl. Acad. Sci. U.S.A. 1996; 93:11919–11924. [PubMed: 8876238]
6. Telenti A, Philipp WJ, Sreevatsan S, Bernasconi C, Stockbauer KE, Wieles B, Musser JM, Jacobs WR Jr. The *emb.* operon, a gene cluster of *Mycobacterium tuberculosis* involved in resistance to ethambutol. Nat. Med. 1997; 3:567–570. [PubMed: 9142129]
7. Takayama K, Wang L, David HL. Effect of isoniazid on the in vivo mycolic acid synthesis, cell growth, and viability of *Mycobacterium tuberculosis*. Antimicrob. Agents Chemother. 1972; 2:29–35. [PubMed: 4208567]
8. Schroeder EK, de Souza ON, Santos DS, Blanchard JS, Basso LA. Drugs that inhibit mycolic acid biosynthesis in *Mycobacterium tuberculosis*. Curr. Pharm. Biotech. 2002; 3:197–225.
9. Takayama K, Wang C, Besra GS. Pathway to synthesis and processing of mycolic acids in *Mycobacterium tuberculosis*. Clin. Microbiol. Rev. 2005; 18:81–101. [PubMed: 15653820]
10. Fukui Y, Hirai T, Uchida T, Yoneda M. Extracellular proteins of tubercle bacilli. IV. Alpha and beta antigens as major extracellular protein products and as cellular components of a strain (H37Rv) of *Mycobacterium tuberculosis*. Biken J. 1965; 8:189–199. [PubMed: 4955992]
11. Kilburn JO, Takayama K, Armstrong EL. Synthesis of trehalose dimycolate (cord factor) by a cell-free system of *Mycobacterium smegmatis*. Biochem. Biophys. Res. Commun. 1982; 108:132–139. [PubMed: 7150277]
12. Sathyamoorthy N, Takayama K. Purification and characterization of a novel mycolic acid exchange enzyme from *Mycobacterium tuberculosis*. J. Biol. Chem. 1987; 262:13417–13423. [PubMed: 3654621]
13. Jackson M, Raynaud C, Laneelle M-A, Guilhot C, Laurent-Winter C, Ensergueix D, Gicquel B, Daffe M. Inactivation of the antigen 85C gene profoundly affects the mycolate content and alters the permeability of the *Mycobacterium tuberculosis* cell envelop. Mol. Microbiol. 1999; 31:1573–1587. [PubMed: 10200974]
14. Puech V, Bayan N, Salim K, Leblon G, Daffé M. Characterization of the in vivo acceptors of the mycoloyl residues transferred by the corynebacterial PS1 and the related mycobacterial antigens 85. Mol. Microbiol. 2000; 35:1026–1041. [PubMed: 10712685]
15. Belisle JT, Vissa VD, Sievert T, Takayama K, Brennan PJ, Besra GS. Role of the major antigen of *Mycobacterium tuberculosis* in cell wall biogenesis. Science. 1997; 276:1420–1422. [PubMed: 9162010]
16. Harth G, Horwitz MA, Tabatadze D, Zamecnik PC. Targeting the *Mycobacterium tuberculosis* 30/32kDa mycolyl transferase complex as a therapeutic strategy against tuberculosis: Proof of principle using antisense technology. Proc. Natl. Acad. Sci. U.S.A. 2002; 99:15614–15619. [PubMed: 12427974]
17. Harth G, Zamecnik PC, Tabatadze D, Pierson K, Horwitz MA. Hairpin extensions enhance the efficacy of mycolyl transferase-specific antisense oligonucleotides targeting *Mycobacterium tuberculosis*. Proc. Natl. Acad. Sci. U.S.A. 2007; 104:7199–7204. [PubMed: 17438292]
18. Nguyen L, Pieters J. Mycobacterial subversion of chemotherapeutic reagents and host defense tactics: challenges in tuberculosis drug development. Annu. Rev. Pharmacol. Toxicol. 2009; 49:427–453. [PubMed: 19281311]
19. Gobec S, Plantan I, Mravljak J, Ŝavajger U, Wilson RA, Besra GS, Soares SL, Appelberg R, Kikelj D. Design, synthesis, biochemical evaluation and antimycobacterial action of phosphonate inhibitors of antigen 85C, a crucial enzyme involved in biosynthesis of the mycobacterial cell wall. Eur. J. Med. Chem. 2007; 42:54–63. [PubMed: 17010479]

20. Kremer L, Maughan WN, Wilson RA, Dover LG, Besra GS. The *M. tuberculosis* antigen 85 complex and mycolyltransferase activity. Lett. Appl. Microbiol. 2002; 34:233–237. [PubMed: 11940150]
21. Wang J, Elchert B, Hui Y, Takemoto JY, Bensaci M, Wennergren J, Chang H, Rai R, Chang C-WT. Synthesis of trehalose-based compounds and study of their antibacterial activity against *Mycobacterium smegmatis*. Bioorg. Med. Chem. 2004; 12:6397–6413. [PubMed: 15556758]
22. Rose JD, Maddry JA, Comber RN, Suling WJ, Wilson LN, Reynolds RC. Synthesis and biological evaluation of trehalose analogs as potential inhibitors of mycobacterial cell wall biosynthesis. Carbohydr. Res. 2002; 337:105–120. [PubMed: 11814442]
23. Barry CS, Backus KM, Barry CE III, Davis BG. ESI-MS Assay of *M. tuberculosis* cell wall Antigen 85 enzymes permits substrate profiling and design of a mechanism-based inhibitor. J. Am. Chem. Soc. 2011; 133:13232–13235. [PubMed: 21776980]
24. Kam BL, Barascut J-L, Imbach J-L. A general method of synthesis and isolation, and an NMR spectroscopic study, of tetra-*O*-acetyl-D-aldopentofuranose. Carbohydr. Res. 1979; 69:135–142.
25. Ayers JD, Lowary TL, Morehouse CB, Besra GS. Synthetic arabinofuranosyl oligosaccharides as mycobacterial arabinosyltransferase substrates. Bioorg. Med. Chem. Lett. 1998; 8:437–442. [PubMed: 9871594]
26. Sanki AK, Boucau J, Srivastava P, Adams SS, Ronning DR, Sucheck SJ. Synthesis of methyl 5-*S*-alkyl-5-thio-arabinofuranosides and evaluation of their antimycobacterial activity. Bioorg. Med. Chem. 2008; 16:5672–5682. [PubMed: 18450455]
27. Boucau J, Sanki AK, Voss BJ, Sucheck SJ, Ronning DR. A coupled assay measuring *Mycobacterium tuberculosis* antigen 85C enzymatic activity. Anal. Biochem. 2009; 385:120–127. [PubMed: 18992216]
28. Sanki AK, Boucau J, Umesiri FE, Ronning DR, Sucheck SJ. Design, synthesis and biological evaluation of sugar-derived esters, alpha-ketoesters and alpha-ketoamides as inhibitors for *Mycobacterium tuberculosis* antigen 85C. Mol. BioSyst. 2009; 5:945–956. [PubMed: 19668859]
29. Ronning DR, Vissa V, Besra GS, Belisle JT, Sacchettini JC. *Mycobacterium tuberculosis* antigen 85A and 85C structures confirm binding orientation and conserved substrate specificity. J. Biol. Chem. 2004; 279:36771–36777. [PubMed: 15192106]
30. Anderson DH, Harth G, Horwitz MA, Eisenberg D. An interfacial mechanism and a class of inhibitors inferred from two crystal structures of the *Mycobacterium tuberculosis* 30 kDa major secretory protein (Antigen 85B), a mycolyl transferase. J. Mol. Biol. 2001; 307:671–681. [PubMed: 11254389]
31. Goulding CW, Perry LJ, Anderson D, Sawaya MR, Cascio D, Apostol MI, Chan S, Parseghian A, Wang S-S, Wu Y, Cassano V, Gill HS, Eisenberg D. Structural genomics of *Mycobacterium tuberculosis*: a preliminary report of progress at UCLA. Biophys. Chem. 2003; 105:361–370. [PubMed: 14499904]
32. Tonge PJ. Another brick in the wall. Nat. Struct. Biol. 2000; 7:94–96. [PubMed: 10655605]
33. Ronning DR, Klabunde T, Besra GS, Vissa VD, Belisle JT, Sacchettini JC. Crystal structure of the secreted form of antigen 85C reveals potential targets for mycobacterial drugs and vaccines. Nat. Struct. Biol. 2000; 7:141–146. [PubMed: 10655617]
34. Sanki AK, Boucau J, Ronning DR, Sucheck SJ. Antigen 85C-mediated acyl transfer between synthetic acyl donors and fragments of the arabinan. Glycoconj. J. 2009; 5:589–596. [PubMed: 19052863]
35. Umesiri FE, Sanki AK, Boucau J, Ronning DR, Sucheck SJ. Recent advances toward the inhibition of mAG and LAM synthesis in *Mycobacterium tuberculosis*. Med. Res. Rev. 2010; 30:290–326. [PubMed: 20099253]
36. Amemiya Y, Terada A, Wachi K, Miyazawa H, Hatakeyama N, Matsuda K, Oshima T. Synthesis and thromboxane synthetase inhibitory activity of di- or tetrahydrobenzo[*b*]thiophenecarboxylic acid derivatives. J. Med. Chem. 1989; 32:1265–1272. [PubMed: 2724299]
37. Bilokin YV, Vasylyev MV, Branytska OV, Kovalenko SM, Chernykh VP. A novel and expedient approach to new heterocycles containing benzothiophene, benzothieno[2,3-d]pyrimidine and coumarin moieties. Tetrahedron. 1999; 55:13757–13766.

38. Baraldi PG, Romagnoli R, Pavani MG, Nunez MC, Tabrizi MAg, Shryock JC, Leung E, Moorman AR, Uluoglu C, Iannotta V, Merighi S, Borea PA. Synthesis and biological effects of novel 2-amino-3-naphthoylthiophenes as allosteric enhancers of the A_1 adenosine receptor. J. Med. Chem. 2003; 46:794–809. [PubMed: 12593659]

39. Bishop AC, Blair ER. A gatekeeper residue for inhibitor sensitization of protein tyrosine phosphatases. Bioorg. Med. Chem. Lett. 2006; 16:4002–4006. [PubMed: 16716588]

40. Kaila N, Janz K, Huang A, Moretto A, DeBernardo S, Bedard PW, Tam S, Clerin V, Keith JC Jr, Tsao DHH, Sushkova N, Shaw GD, Camphausen RT, Schaub RG, Wang Q. 2-(4-Chlorobenzyl)-3-hydroxy-7,8,9,10-tetrahydrobenzo[H]quinoline-4-carboxylic acid (PSI-697): Identification of a clinical candidate from the quinoline salicylic acid series of P-selectin antagonists. J. Med. Chem. 2007; 50:40–64. [PubMed: 17201409]

41. Sanki, AK.; Sucheck, SJ.; Ronning, DR.; Boucau, J.; Umesiri, FE.; Ibrahim, DA. Inhibitors of Antigen 85 from *Mycobacterium tuberculosis*. Abstracts of Papers, 239th ACS National Meeting; San Francisco, CA, United States. March 21–25; 2010. ORGN-118.

42. Ibrahim, DA.; Adams, SS.; Sucheck, SJ.; Trabbic, KR.; Ronning, DR.; Sanki, AK.; Boucau, J. Inhibitors of *Mycobacterium tuberculosis* Antigen 85. Abstracts, 41st Central Regional Meeting of the ACS; Dayton, OH, United States. June 16–19; 2010. CERMACS-307.

43. Scheich C, Puetter V, Schade M. Novel small molecule inhibitors of MDR *Mycobacterium tuberculosis* by NMR fragment screening of antigen 85C. J. Med. Chem. 2010; 53:8362–8367.

44. Warrier T, Tropis M, Werngren J, Diehl A, Gengenbacher M, Schlegel B, Schade M, Oschkinat H, Daffe M, Hoffner S, Eddine AN, Kaufmann SHE. Antigen 85C inhibition restricts *Mycobacterium tuberculosis* growth through disruption of Cord Factor biosynthesis. Antimicrob. Agents Chemother. 2012; 56:1735–1743. [PubMed: 22290959]

45. Otwinowski Z, Minor W. Processing of X-ray diffraction data collected in oscillation mode. Methods Enzymol. 1997; 276:307–326.

46. Kissinger CR, Gehlhaar DK, Fogel DB. Rapid automated molecular replacement by evolutionary search. Acta Crystallogr D, Biol. Crystallogr. 1999; 55:484–491. [PubMed: 10089360]

47. Emsley P, Lohkamp B, Scott WG, Cowtan K. Features and development of Coot. Acta Crystallogr. D Biol. Crystallogr. 2010; 66:486–501. [PubMed: 20383002]

48. Adams PD, Gopal K, Grosse-Kunstleve RW, Hung LW, Ioerger TR, McCoy AJ, Moriarty NW, Pai RK, Read RJ, Romo TD, Sacchettini JC, Sauter NK, Storoni LC, Terwilliger TC. Recent developments in the PHENIX software for automated crystallographic structure determination. J. Synchrotron Radiat. 2004; 11:53–55. [PubMed: 14646133]

49. Adams PD, Grosse-Kunstleve RW, Hung LW, Ioerger TR, McCoy AJ, Moriarty NW, Read RJ, Sacchettini JC, Sauter NK, Terwilliger TC. PHENIX: building new software for automated crystallographic structure determination. Acta Crystallogr. D Biol. Crystallogr. 2002; 58:1948–1954. [PubMed: 12393927]

50. Performance standards for antimicrobial disk susceptibility tests. 7th ed.. Wayne, Pa: National Committee for Clinical Laboratory Standards; 2000. National Committee for Clinical Laboratory Standards. Approved Standard: M2-A7.

51. Peet NP, Sunder S, Barbuch RJ, Vinogradoff AP. Mechanistic observations in the Gewald syntheses of 2-aminothiophene. J. Heterocycl. Chem. 1986; 23:129–134.

52. Gewald K, Schinke E, Böttcher H. Heterocyclen aus CH-aciden nitrilen, VIII. 2-Amino-thiophene aus methylenaktiven nitrilen, carbonylverbindungen und schwefel. Chem. Ber. 1966; 99:94–100.

53. Khan KM, Nullah Z, Lodhi MA, Jalil S, Choudhary MI, Rahman AU. Synthesis and anti-inflammatory activity of some selected aminothiophene analogs. J. Enzym. Inhib. Med. Chem. 2006; 21:139–143.

54. Manhas MS, Rao VV, Amin SGJ. Heterocyclic compounds. VII. Synthesis of thiadiazasteroid analogs. Heterocycl. Chem. 1976; 13:821–824.

55. Hagen, H.; Nilz, G.; Walter, H.; Landes, A. Preparation of 2-aminothiophene derivatives as herbicide antidotes. United States Patent. 5,442,335. 1995 Jun 6.

56. Sugiyama M, Sakamoto T, Tabata K, Endo K, Ito K, Kobayashi M, Fukumi H. Condensed thienopyrimidines. I. Synthesis and gastric antisecretory activity of 2,3-dihydro-5H-

oxazolothienopyrimidin-5-one derivatives. Chem. Pharm. Bull. 1989; 37:2091–2102. [PubMed: 2598309]

57. Yoshimura Y, Kuze T, Ueno M, Komiya F, Haraguchi K, Tanaka H, Kano F, Yamada K, Asami K, Kaneko N, Takahata H. A Practical synthesis of 4'-thioribonucleosides. Tetrahedron Lett. 2006; 47:591–594.
58. Hughes NA, Kuhajda K-M, Miljkovic DA. New syntheses of methyl 5-thio-β-D-arabinopyranoside and (+) biotin. Carbohydr. Res. 1994; 257:299–304.
59. Friesner RA, Banks JL, Murphy RB, Halgren TA, Klicic JJ, Mainz DT, Repasky MP, Knoll EH, Shelley M, Perry JK, Shaw DE, Francis P, Shenkin PS. Glide: A new approach for rapid, accurate docking and scoring. 1. Method and assessment of docking accuracy. J. Med. Chem. 2004; 47:11729–11749.
60. Jacobson MP, Pincus DL, Rapp CS, Day TJ, Honig B, Shaw DE, Friesner RA. A hierarchical approach to all-atom protein loop prediction. Proteins. 2004; 55:351–367. [PubMed: 15048827]
61. Kaminski GA, Friesner RA, Tirado-Rives J, Jorgensen WLJ. Evaluation and reparametrization of the OPLS-AA force field for proteins via comparison with accurate quantum chemical calculations on peptides. Phys. Chem. B. 2001; 105:6474–6487.
62. Yu Z, Jacobson MP, Friesner RA. What role do surfaces play in GB models? A new-generation of surface-generalized born model based on a novel Gaussian surface for biomolecules. J. Comput. Chem. 2006; 27:72–89. [PubMed: 16261581]
63. García-lópez J, Hernández-Mateo F, Isac-García J, Kim J, Roy R, Santoyo-González F, Vergas-Berengeul A. Synthesis of per-glycosylated β-cyclodextrines having enhanced lectin binding affinity. J. Org. Chem. 1999; 64:522–531.
64. Skaanderup PR, Poulsen CS, Hyldtoft L, Jorgensen MR, Madsen R. Regioselective conversion of primary alcohols into iodides in unprotected methyl furanosides and pyranosides. Synthesis. 2002; 12:1721–1727.

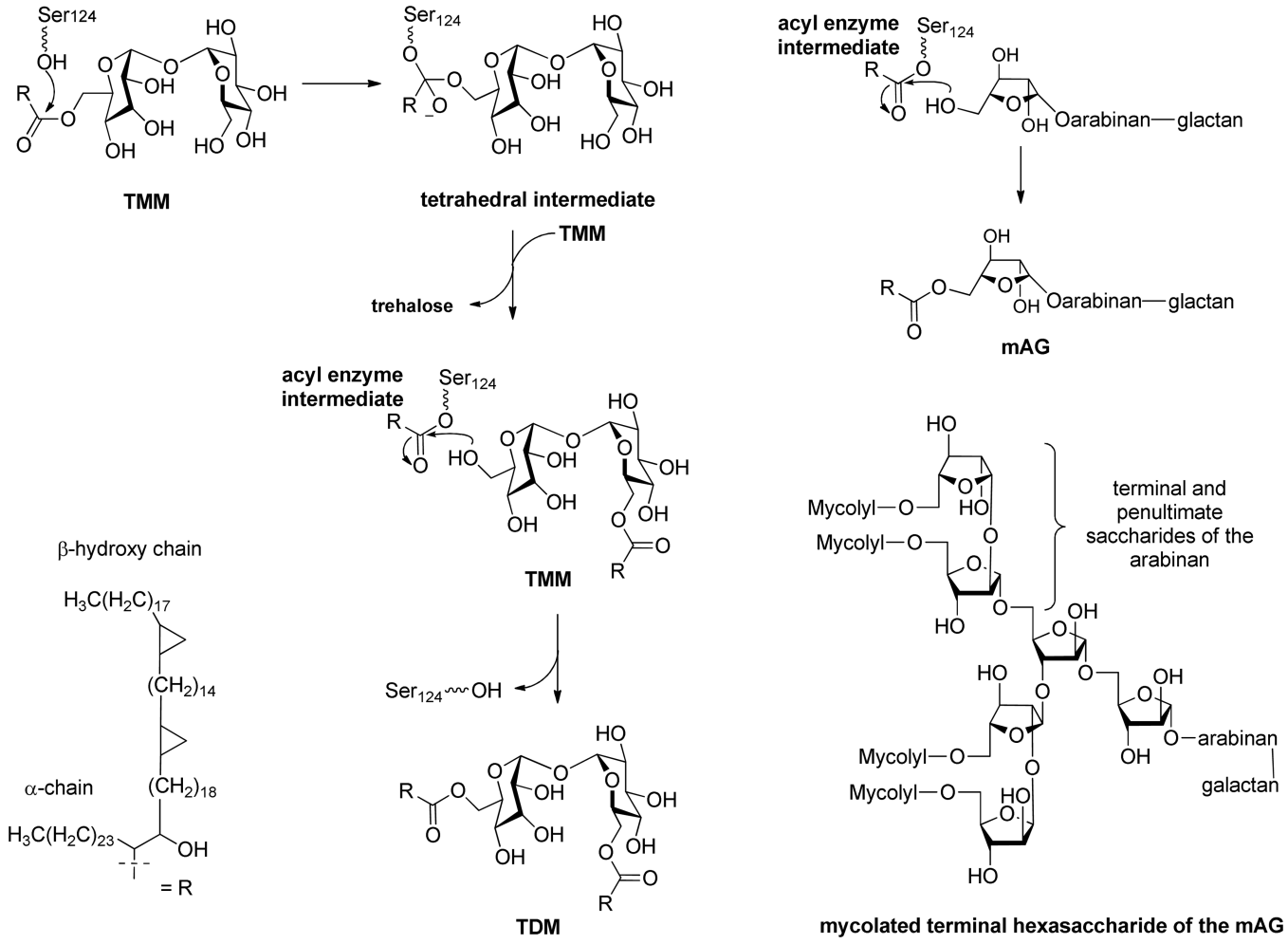

Figure 1.
Proposed mechanism for Ag85-mediated mycolyl transfer resulting in the formation of mAG and TDM.

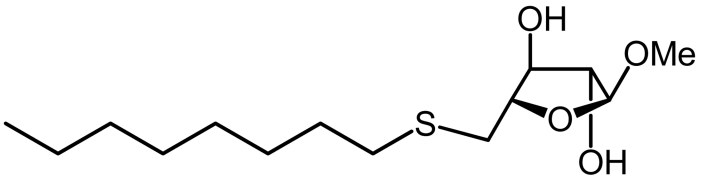

S-alkyl arabinofuranosides

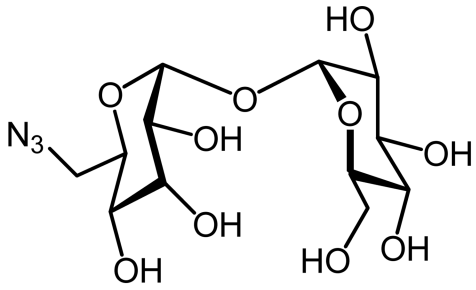

6-azido-6-deoxytrehalose

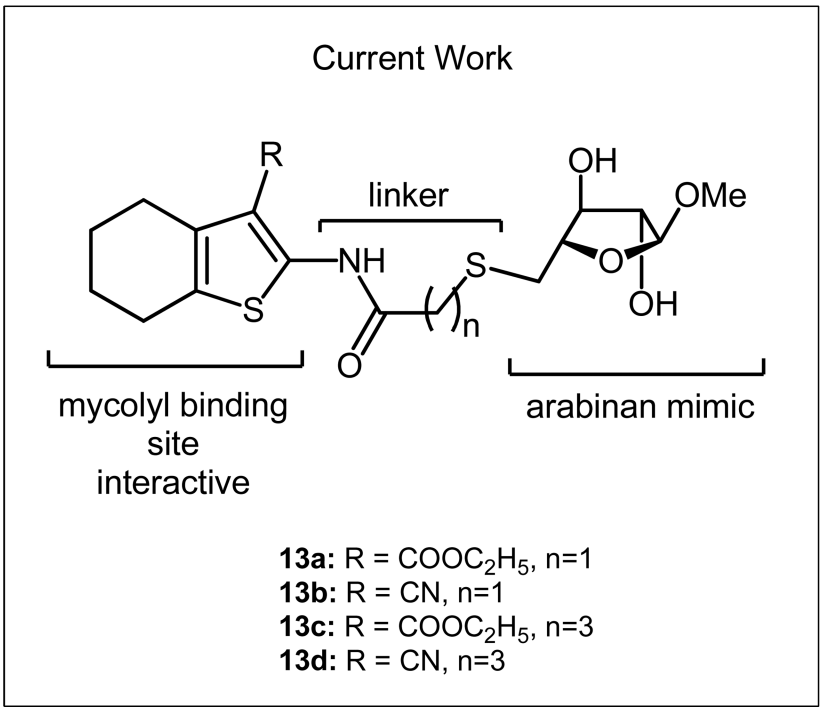

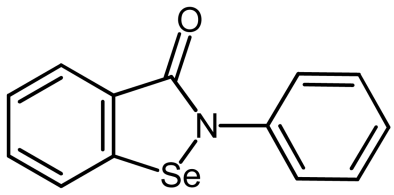

ebselen

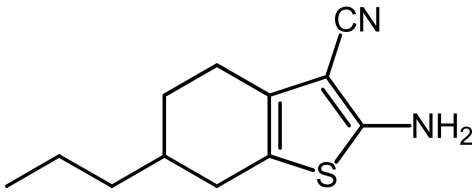

I3-AG85

Figure 2.
Design of arbinose-thiophene conjugates designed to act as inhibitors of Ag85s. Structures of an *S*-alkyl arabinofuranoside, ebselen and I3-AG85.

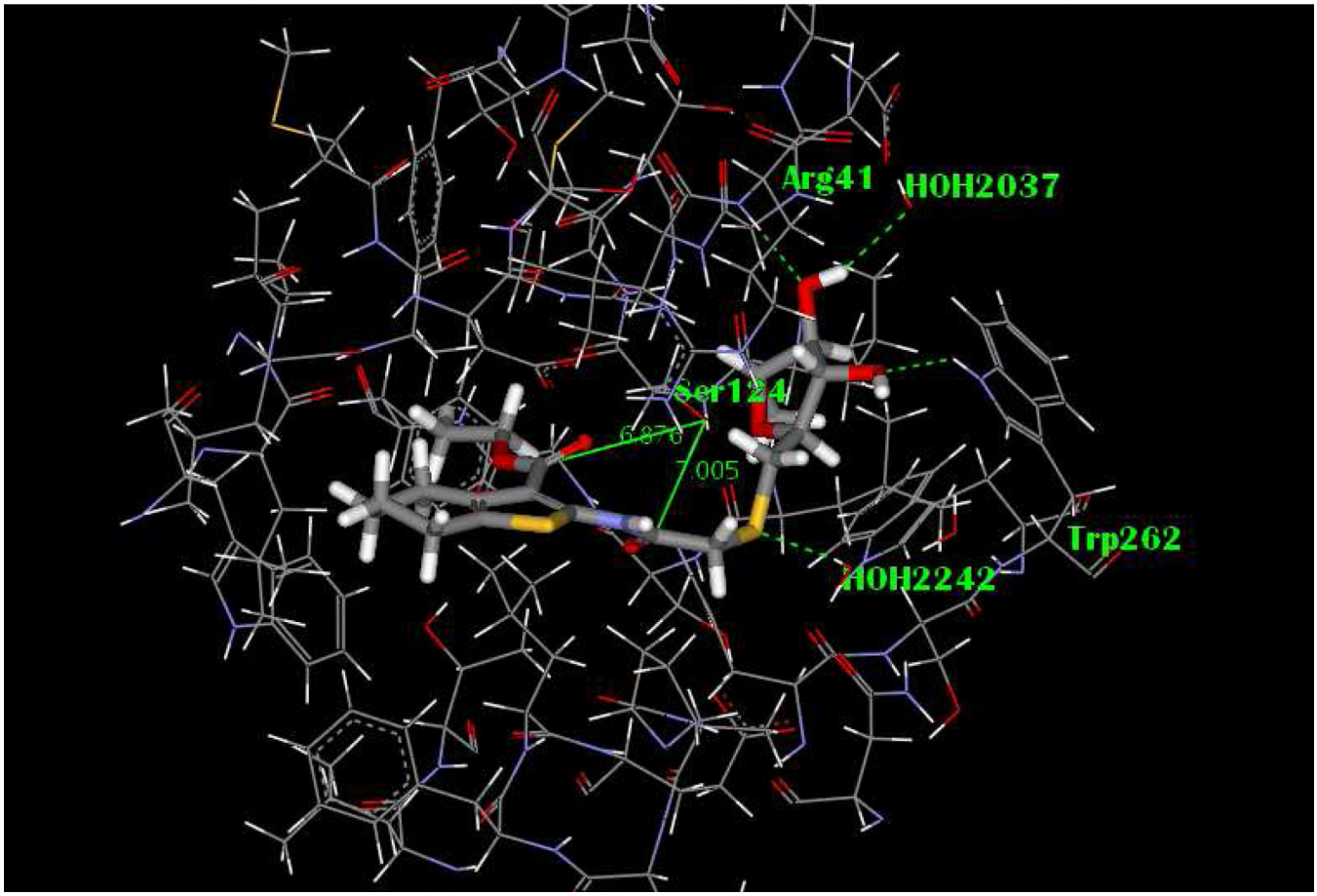

Figure 3.
Hypothetical binding mode of inhibitor **13a** in the Ag85C active site predicted using Glide 4.5. The arabinofuranoside substituent is located in the trehalose binding pocket and the ester moiety is oriented in the vicinity of Ser124. The tetrahydrobenzo[*b*]thiopene is accommodated in the mycolate α-chain binding channel extending through the core of Ag85C.

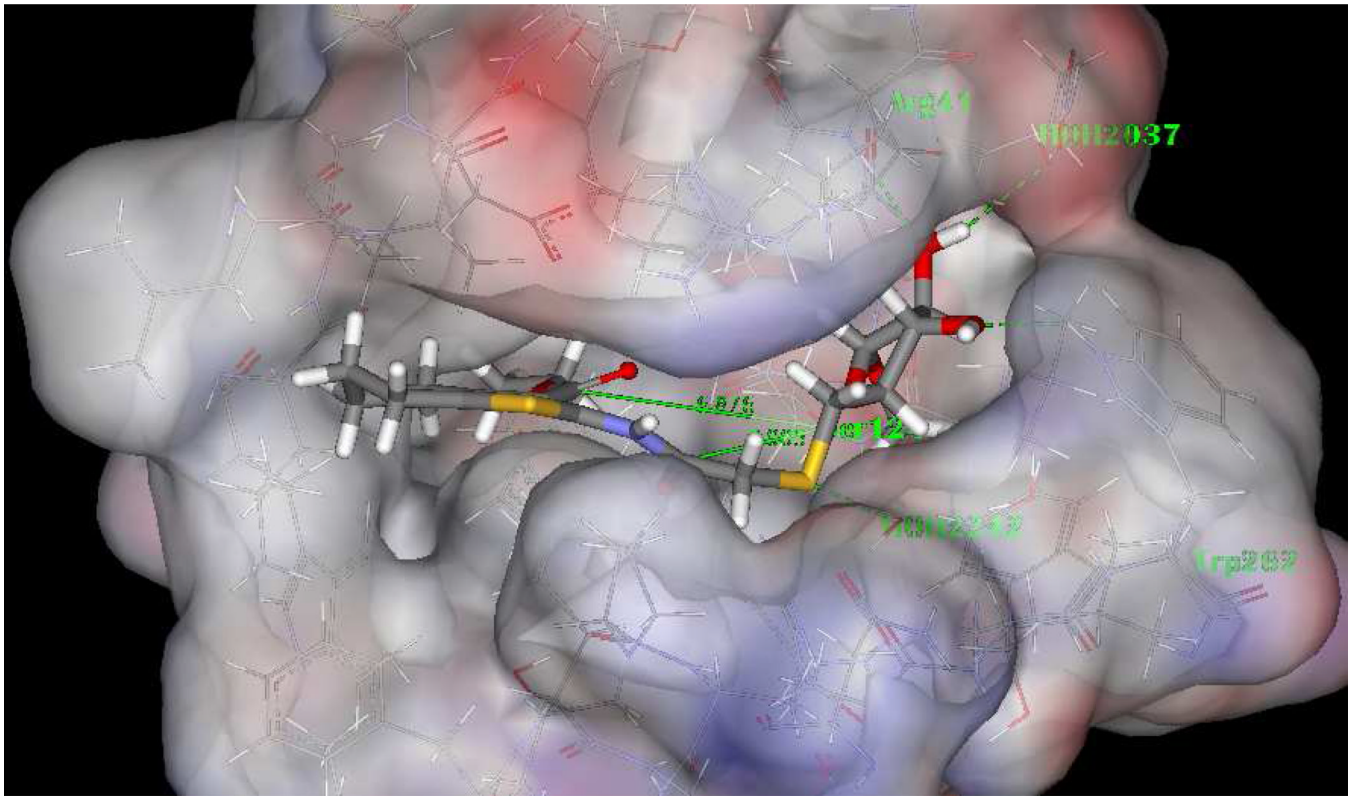

Figure 4.
The electrostatic potential and hydrogen bonding interaction between compound **13a** and Ag85C. The distances between the OH of Ser124 and the ester and amide C=O moieties of **13a** is indicated by green lines.

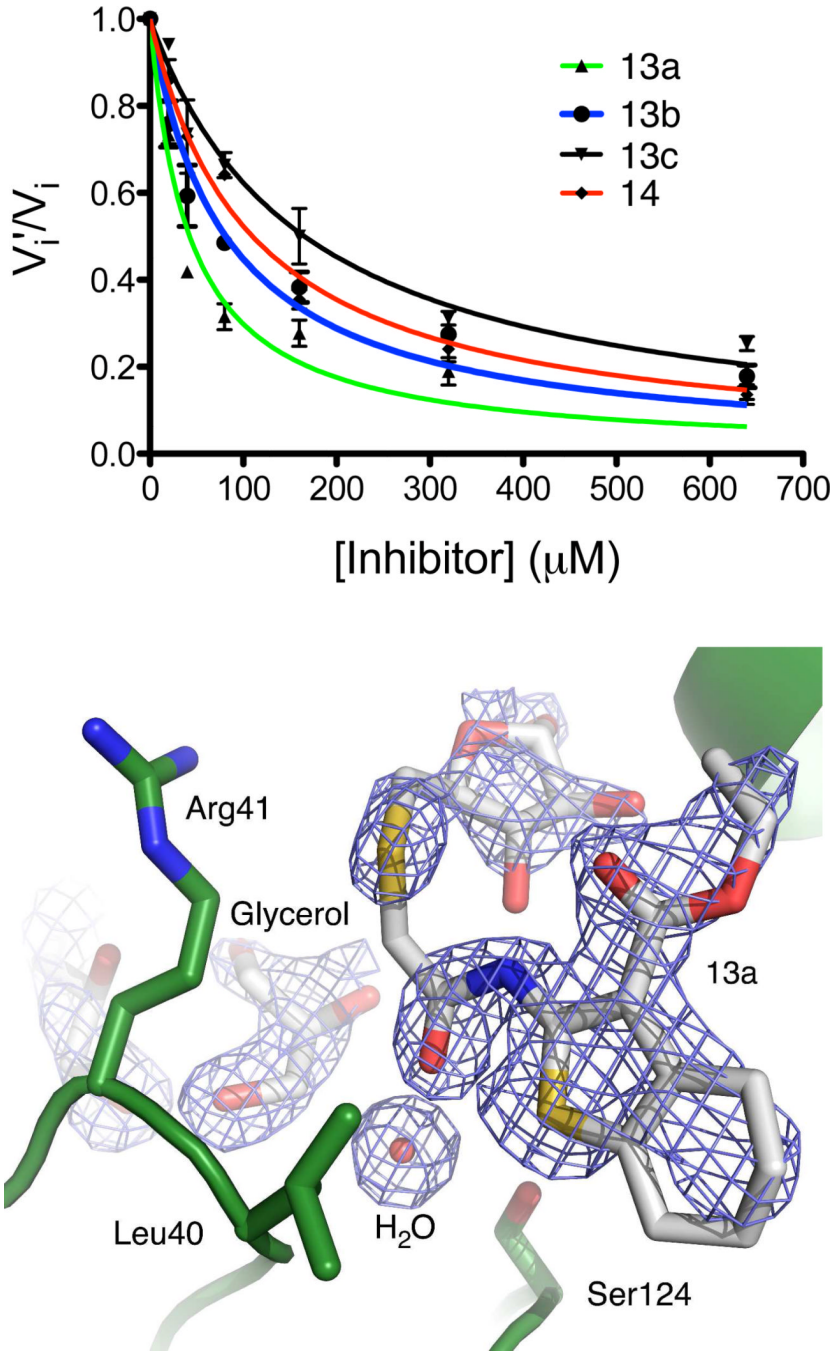

Figure 5.

Inhibition of Ag85C. A) v_i' represents the initial velocity of the inhibited enzymatic reaction at the respective inhibitor concentration. v_i represents the initial velocity of the uninhibited enzymatic reaction. B) The enzyme active site is shown (with green carbon atoms) with one molecule of **13a**, one water molecule, and two molecules of glycerol (molecules with gray carbon atoms). The placement of these compounds was based on the F_o-F_c omit maps (light blue difference density) shown contoured at 3σ. Colors for the atoms other than carbon are blue, red, and yellow for nitrogen, oxygen, and sulfur, respectively.

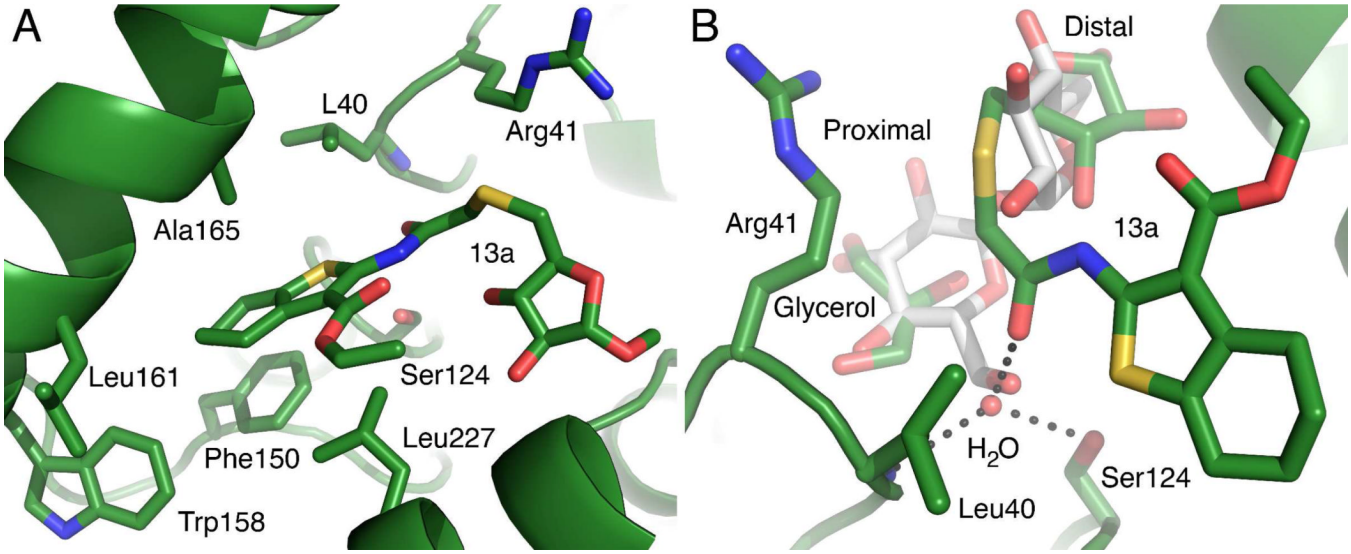

Figure 6.

Interactions between **13a** and the Ag85C active site. Two views of the Ag85C active site are shown from different orientations A) Non-specific interactions. The Ag85C protein backbone is shown as the green ribbon. The carbon atoms are in green, nitrogen atoms are in blue, oxygen in red and sulfur in yellow. The location of the serine nucleophile is shown as a reference. All of the hydrophobic residues within 4 Å of the thiophene moiety are shown as well as the R41 side chain that interacts with the thioether linker. B) The superposition of the trehalose-bound Ag85B and the **13a**-bound Ag85C structures shows overlap of the trehalose and **13a** binding sites. The trehalose from the Ag85B structure is shown with gray carbon atoms. All other atom types are colored as in panel A. The distal glucosyl moiety of trehalose and the methylarabinoside of **13a** are clearly occupying the same region within the active site. The proximal glucosyl and an ordered glycerol molecule also superimpose well and form similar hydrogen bonding interactions with Ag85. The ordered water molecule near O6 of the Ag85b-bound trehalose is shown. The dashed lines represent hydrogen bonds between this water molecule and the **13a** amide carbonyl, the side chain of Ser124, and the backbone amide of Leu40, which forms part of the oxyanion hole. The length of these hydrogen bonds range from 2.6 to 3.0 Å.

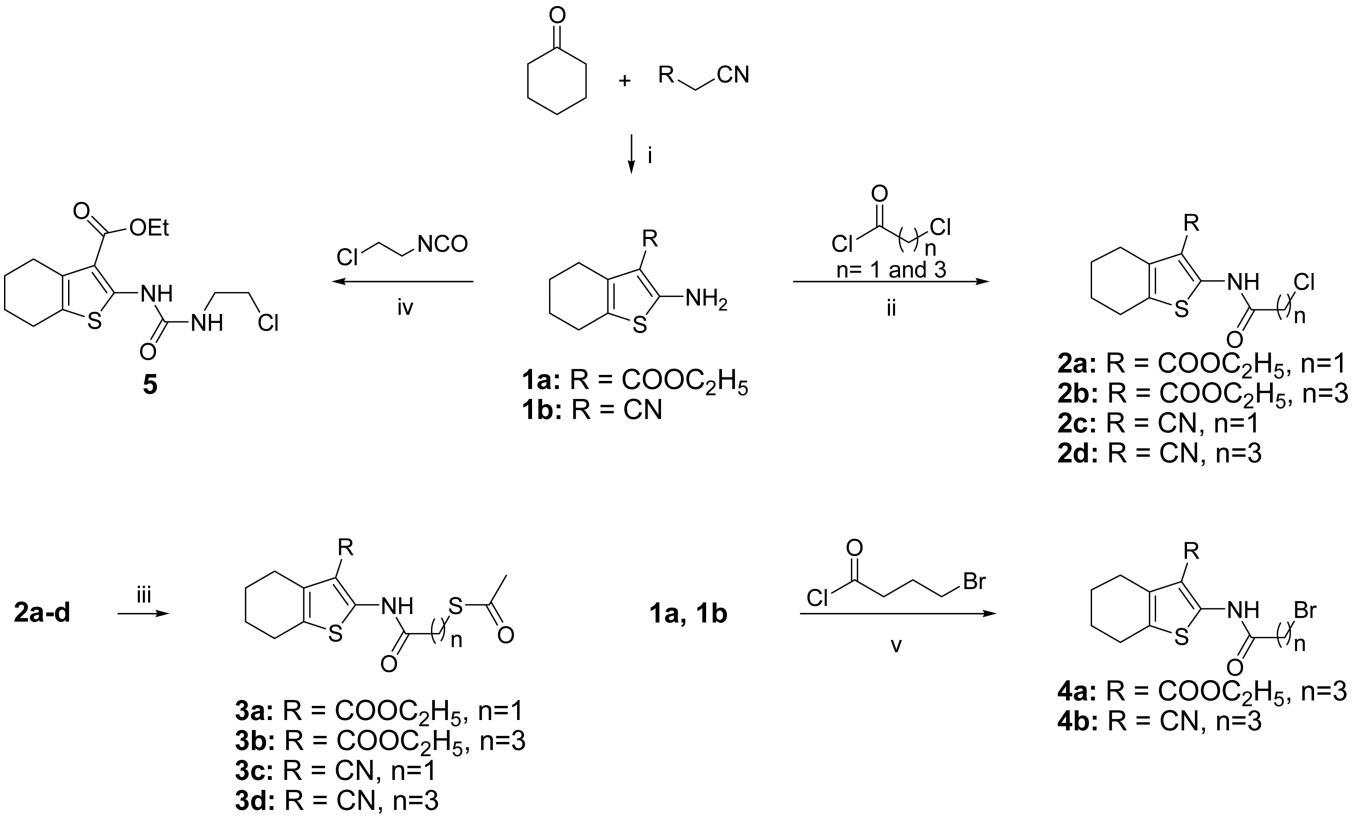

Scheme 1.

Synthesis of Tetrahydrobenzo[*b*]thiophenesa

[a]Reagent and conditions: (i): sulfur, *N*-ethylmorpholine, EtOH, **1a** (27%), **1b** (33%); (ii): Et_3N, CH_2Cl_2, rt, **2a** (11%), **2b** (9%), **2c** (15%), **2d** (29%); (iii): $KSCOCH_3$, DMF, rt, **3a** (62%), **3b** (66%), **3c** (96%), **3d** (78%); (iv) toluene, 112 °C, 3 h (53%); (v): CH_2Cl_2, rt, **4a** (39%), **4b** (67%).

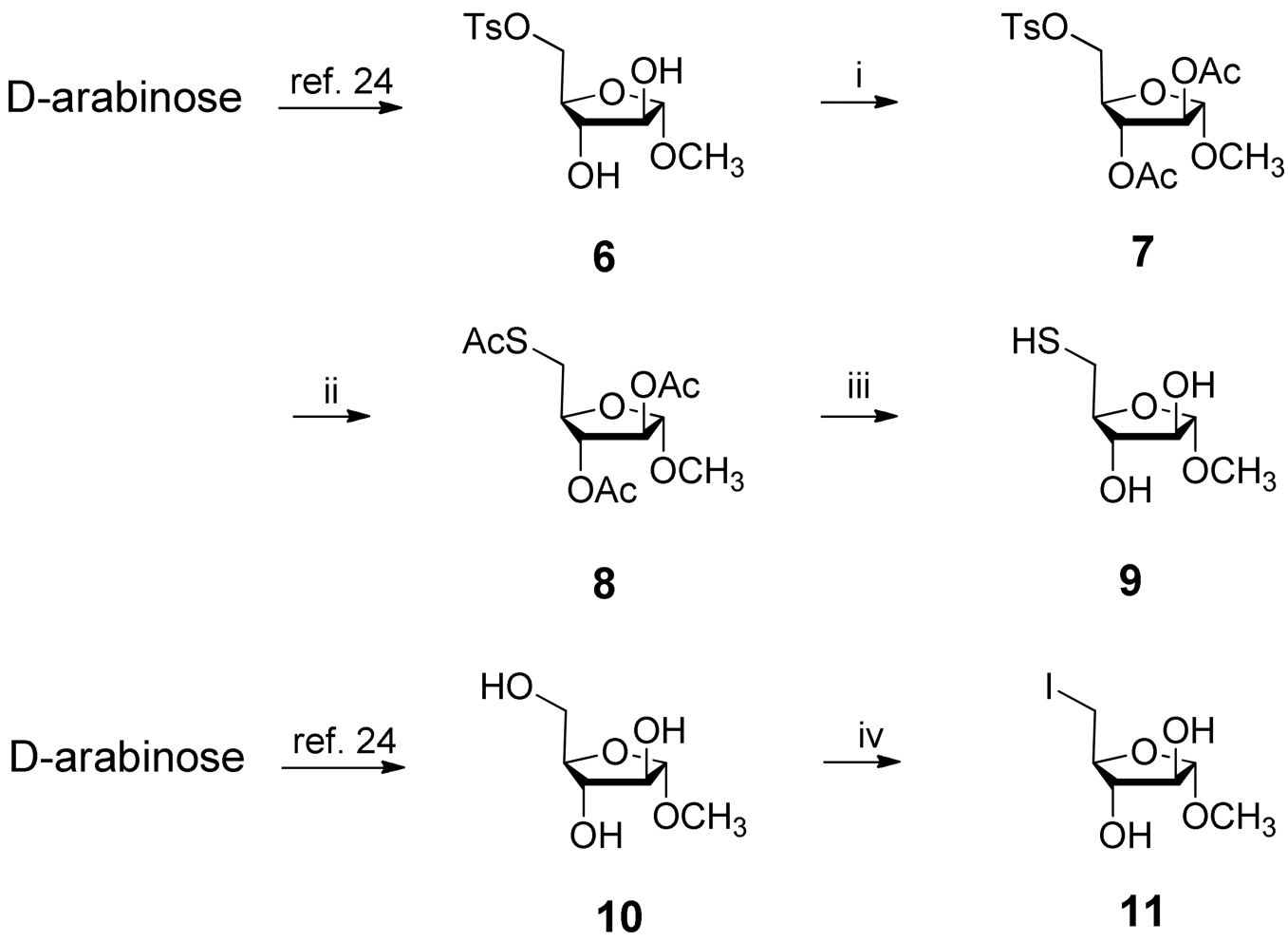

Scheme 2.

Synthesis of Arabinofuranosides a

[a]Reagent and conditions: (i): Ac_2O, pyridine, 24 h, rt (73%); (ii): $KSCOCH_3$, DMF, 24 h, rt (60%); (iii) 0.1 M methanolic NaOMe 2 h, 50 °C then Amberlite™ IR120; (iv) imidazole, I_2, PPh_3, THF, 0 to 65 °C, (65 %).

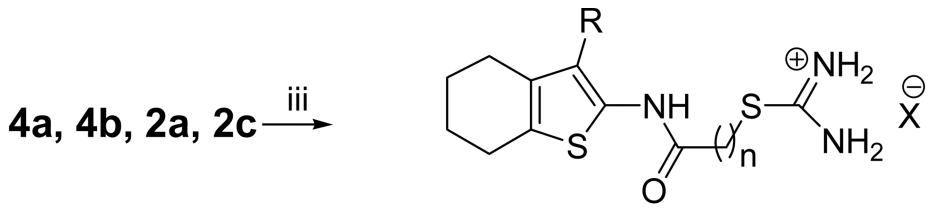

12a: R = $COOC_2H_5$, n=1, X=Cl
12b: R = CN, n=1, X=Cl
12c: R= $COOC_2H_5$, n=3, X=Br
12d: R=CN, n=3, X=Br

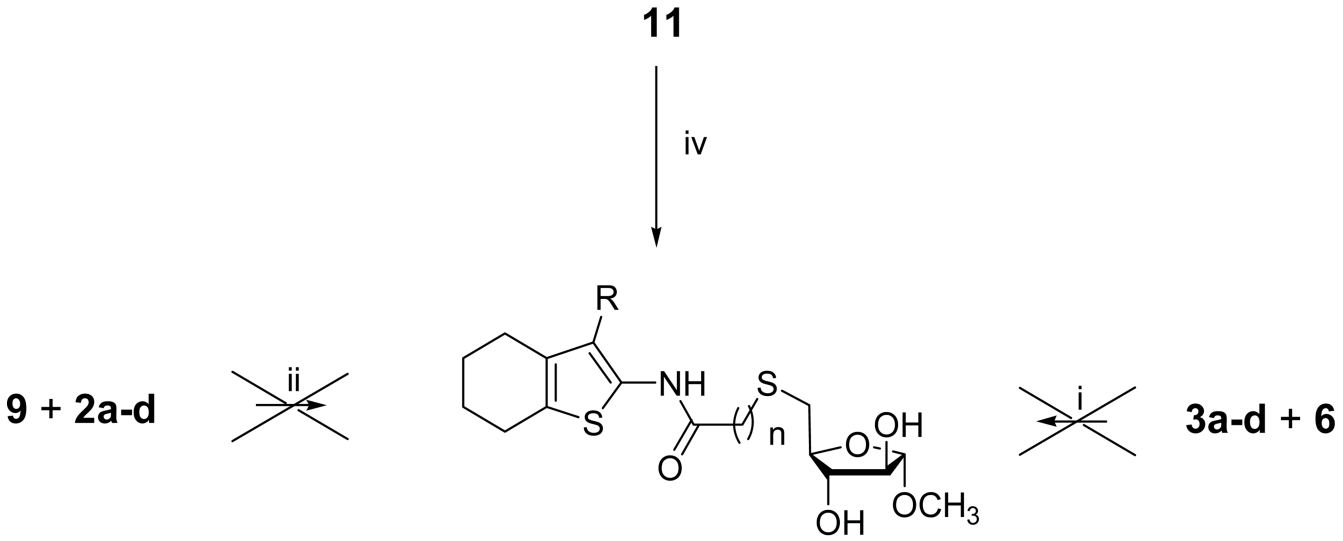

13a: R = $COOC_2H_5$, n=1
13b: R = CN, n=1
13c: R = $COOC_2H_5$, n=3
13d: R = CN, n=3

Scheme 3.
Isothiourionium Salt Based-synthesis of Thioethers a
[a]Reagent and conditions: (i): NaOEt, MeOH, rt, no reaction; (ii) THF, TEA, 6 h, rt, no reaction; (iii) $CS(NH_2)_2$, EtOH, 4 h, reflux, **12a** (83%), **12b** (80%), **12c** (52 %), **12d** (71%); (iv) **12a -12d**, Cs_2CO_3, DMF, 16 h, 85 °C, **13a** (28%), **13b** (56%), **13c** (77%), **13d** (49%).

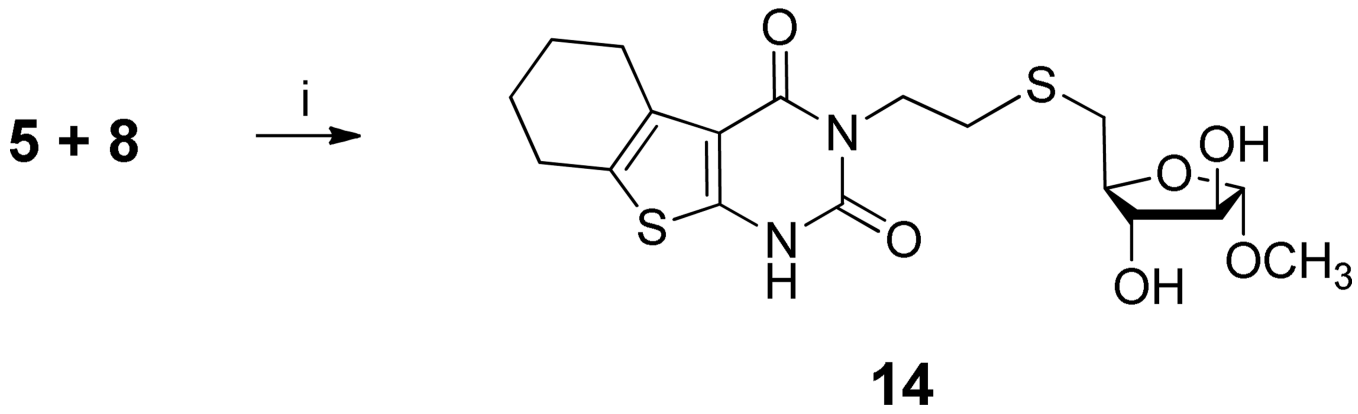

14

Scheme 4.
Synthesis of Pyrimidinedione 14
[a]Reagents and conditions: (i): NaOMe, MeOH, 24h, rt (13 %).

Table 1

Docking Scores, Binding Energies, and Measured K_i of Compounds 13a–d and Compound 14

Compound	Docking Score	Binding Energy	K_i (μM) [a]
Native Ligand	−11.3	−53	N.D.
13a	−12	−62	18.2 +/−1.8
13b	−12.88	−19	34.8 +/−3.8
13c	−11.4	−6	71.0 +/−5.3
13d	−10.9	−29	N.D.
14	−11.85	−15	47.1 +/−3.9

[a] N.D. = no data.

Table 2

X-ray Diffraction and Crystallographic Refinement Data

Diffraction Statistics	
Resolution range (Å) (highest shell)	35-2.15 (2.20–2.15)
Space Group	$P2_12_12_1$
Unit cell parameters	a=67.5,b=80.2,c=136.6, α=β=γ=90°
Total reflections (unique reflections)	246,157 (40,674)
Completeness (%) (highest shell)	99.0 (99.9)
Average I/σI	7.0
Rsym (%) (highest shell)	8.8 (40.4)
Refinement Statistics	
Protein Molecules/Atoms (per A.S.U.)	2/4695
Rwork/Rfree (%)	15.86/19.66
Average B-factor (Å ^{2}) (protein/ligand/solvent)	25.66/43.58/36.17
Ligand Occupancy (%)	100
r.m.s.d. bonds/angles (Å/°)	0.007/1.041
Ramachanran (favored/disallowed) (%)	96.2/0.0